AD-A202 018

AFGL-TR-88-0167

Discrimination Using P_n and P_g

L.J. Burdick
C.K. Saikia
N.F. Smith

Woodward-Clyde Consultants
566 El Dorado Street
Suite 100
Pasadena, CA 91101

15 April 1988

Scientific Report No. 2

BEST
AVAILABLE COPY

APPROVED FOR PUBLIC RELEASE; DISTRIBUTION UNLIMITED

DTIC
ELECTE
NOV 21 1988
E

AIR FORCE GEOPHYSICS LABORATORY
AIR FORCE SYSTEMS COMMAND
UNITED STATES AIR FORCE
HANSCOM AIR FORCE BASE, MASSACHUSETTS 01731-5000

88 11 21 011
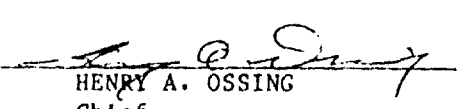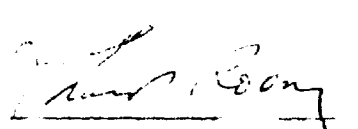
The views and conclusions contained in this document are those of the authors and
should not be interpreted as representing the official policies, either expressed
or implied, of the Defense Advanced Research Projects Agency or the US Government.

"This technical report has been reviewed and is approved for publication"

JAMES F. LEWKOWICZ   HENRY A. OSSING
Contract Manager   Chief
Solid Earth Geophysics Branch   Solid Earth Geophysics Branch
Earth Sciences Division   Earth Sciences Division

FOR THE COMMANDER

THOMAS P. ROONEY, Acting Director
Earth Sciences Division

REPORT DOCUMENTATION PAGE

1a REPORT SECURITY CLASSIFICATION	1b. RESTRICTIVE MARKINGS
Unclassified	

2a SECURITY CLASSIFICATION AUTHORITY	3. DISTRIBUTION/AVAILABILITY OF REPORT
2b DECLASSIFICATION/DOWNGRADING SCHEDULE	Approved for public release; Distribution unlimited.

4 PERFORMING ORGANIZATION REPORT NUMBER(S)	5. MONITORING ORGANIZATION REPORT NUMBER(S)
WCCP-R-88-02	AFGL-TR-88-0167

6a NAME OF PERFORMING ORGANIZATION	6b OFFICE SYMBOL (If applicable)	7a. NAME OF MONITORING ORGANIZATION
Woodward-Clyde Consultants		Air Force Geophysics Laboratory

6c. ADDRESS (City, State, and ZIP Code)	7b. ADDRESS (City, State, and ZIP Code)
566 El Dorado Street, Suite 100 Pasadena, CA 91101	Hanscom Air Force Base Massachusetts 01731-5000

8a. NAME OF FUNDING/SPONSORING ORGANIZATION	8b. OFFICE SYMBOL (If applicable)	9. PROCUREMENT INSTRUMENT IDENTIFICATION NUMBER
DARPA		F1968-87-C-0081

8c ADDRESS (City, State, and ZIP Code)	10. SOURCE OF FUNDING NUMBERS			
	PROGRAM ELEMENT NO.	PROJECT NO.	TASK NO.	WORK UNIT ACCESSION NO.
1400 Wilson Boulevard Arlington, VA 22209	62714E	7A10	DA	DD

11 TITLE (Include Security Classification)

Discrimination Using P_n and P_g (Unclassified)

12 PERSONAL AUTHOR(S)
L.J. Burdick, C. K. Saikia, N. F. Smith

13a. TYPE OF REPORT	13b. TIME COVERED	14. DATE OF REPORT (Year, Month, Day)	15. PAGE COUNT
Scientific Report#2	FROM 9/5/87 TO 3/5/88	1988 April 15	68

16. SUPPLEMENTARY NOTATION

17	COSATI CODES		18. SUBJECT TERMS (Continue on reverse if necessary and identify by block number)
FIELD	GROUP	SUB-GROUP	Regional Discriminants, P_g, P_n, P_{nl}, Synthetic Seismograms

19 ABSTRACT (Continue on reverse if necessary and identify by block number)

See Reverse Side of Page

20 DISTRIBUTION/AVAILABILITY OF ABSTRACT	21. ABSTRACT SECURITY CLASSIFICATION
☒ UNCLASSIFIED/UNLIMITED ☐ SAME AS RPT. ☐ DTIC USERS	Unclassified

22a NAME OF RESPONSIBLE INDIVIDUAL	22b. TELEPHONE (Include Area Code)	22c. OFFICE SYMBOL
James F. Lewkowicz	(617) 377-3028	AFGL/LWH

DD FORM 1473, 84 MAR 83 APR edition may be used until exhausted.   SECURITY CLASSIFICATION OF THIS PAGE
All other editions are obsolete.

BLOCK 19: ABSTRACT

Two regional discriminants are being developed and tested on western U.S. data bases. The first is based on the observation that the onset of the P_n waveform is stable in character and typically much different than most earthquake P_n waveforms. It is fairly similar in shape to teleseismic short period P waveforms and it exhibits the splitting of the second upswing which is associated with the arrival of effective pP. The average waveform was measured at two analog and two digital stations by summing several waveforms together. The results were reasonably consistent between stations. The average waveform at a fixed station is exceptionally consistent between the Pahute Mesa and Yucca test sites indicating that average P_n waveform is a stable function of time. Synthetics were computed both on the assumption that high frequency P_n is a turning ray in a smooth positive gradient in the lid and also that it is a true head wave. The former seems to be a better representation. This would explain the similarity between regional P_n and teleseismic P. The synthetic analysis showed that effective pP is later than elastic time as is usually observed. This implies that effective pP is generated by a more complex process than simple reflection and probably involves spall. A set of earthquake P_n waveforms from the digital stations was collected. It was found that earthquakes could be discriminated from explosions on the basis of the correlation of the P_n waveform with the average explosion P_n. The second discriminant is being developed around the P_g waveform. A suite of explosion P_g's was averaged to find which of its characteristics are most stable. It was found that P_g is composed of a sequence of subpulses which can be shown through synthetic modeling to be associated with successive reverberations of energy in the crust. The first reverberation appears to be a channel for effective P transmission and the second for effective S transmission. The ratio of the amount of S energy contained in them may thus provide the basis for a discriminant.

Seismic Discrimination (jld)

TABLE OF CONTENTS

INTRODUCTION

The time and frequency domains are equivalent displays of seismic trace information, though some qualities of the signal are more easily observed in one domain than the other. The relative frequency excitation of Lg, for instance, is most easily viewed in the frequency domain, but such waveform qualities as the sequence in which pulses arrive in the wave train or the sharpness of pulse onset are most easily studied in the time domain (Murphy and Bennett, 1982; Burdick and Helmberger, 1988; Blandford, 1981). Because of the tremendous complexity of high frequency regional data, most attempts at using it for discrimination purposes have involved analysis of the frequency content of the various arrivals either through transforming selected windows or through multiple bandpass filtering. In this report, we examine the alternative and attempt to discriminate events using those waveform characteristics most easily observed in the time domain.

The greatest difficulty in interpreting short period regional data is that it is so strongly affected by scattering phenomena. The best approach to analyzing it may be to use array processing techniques on data recorded at technically advanced seismic arrays. Such techniques measure the average properties of signals arriving in given velocity windows. In this work, we are attempting to characterize the average properties of some of the more prominent regional phases using fundamental array processing techniques. However, we have reversed the role of sources and stations. We use an array of sources recorded at a single station rather than the converse.

In analyzing a test discrimination data set from the western U. S., we have discovered that the onset of P_n is always very similar for explosions and

1

that few earthquakes have this unique waveform character. We have also discovered that the regional phase P_g is actually composed of a sequence of sub-arrivals which correspond to successively higher orders of reverberation in the crust (Burdick and Helmberger, 1988). The scattering associated with each new reverberation accounts for the long duration and complexity of P_g. We suspect that an analogous set of reverberations with scattering may account for S_g. In analyzing these crustal resonance phases, we found that the first reverberation is dominated by PmP type rays, but the second is not dominated by second multiples of P energy as might have been expected. Rather, it is dominated by waves with at least one converted leg. In viewing high frequency data, we have found that the second resonance phase has markedly different particle motion than the first and that the second phase is much richer in S energy. This suggests that discrimination may be possible through analysis of the evolution of particle motion of P_g with time. We first discuss the P_n discriminant and then the P_g.

THE P_n WAVEFORM DISCRIMINANT

The situation of having data available from many sources very close to each other which are similar in character such as NTS explosions is a unique one. The timing and locations of the events are known exactly. This turns any single regional station in the western U. S. into the equivalent of a regional seismic array. Any of the standard array processing techniques can be used with the role of sources and stations being reversed. There is some variability in source time history and near source structure, but on the other hand the receiver structure is constant. This fact is being exploited in the studies discussed in the following in an attempt to find what properties of regional data are stable enough on average to be used for discrimination purposes. There are a number of high quality regional seismic stations around NTS from which to choose. These include the DWWSSN stations ALQ and JAS, the four broad band LLNL stations and new stations at Pasadena and Pinyon Flat. These last two are instrumented with the state of the art Streckeisens which are installed at Grafenberg and will be installed at the new international stations in the Soviet Union. For this, the exploratory part of the investigation, we simply use those stations for which the data are routinely included on the USGS Network Day Tape. These are the WWSSN stations ALQ and JAS.

To begin the study, data bases of explosion and earthquake signals were assembled from the day tape. The short and long period signals were plotted on expanded time scales and examined for features that tended to discriminate the two source types. In so doing, it was noted that the first few swings of P_n were very consistent in shape and contained a very interesting feature.

Six typical P_n's from Yucca events as observed at ALQ and six others at JAS are shown in Figures 1 and 2. The variation in event size is almost two magnitude units. The signals have the characteristic small upswing, larger downswing and largest second upswing observed in short period explosion P waves at teleseismic distances. The usual nomenclature for them is the "a", "b" and "c" swings respectively. The "a" swing is very emergent at ALQ A feature which could be described as a splitting of the "c" swing is indicated by arrows in the figures. It is more apparent in the higher frequency small events, and, as is also indicated in the figures, we believe it is caused by pP energy. One reason we have for making this inference is illustrated by Figure 3 where we show some of the short and long period teleseismic P waves from the very deep event CANNIKIN. As indicated by the arrows some of the data exhibits the same split "c" swing as observed in the P_n data though it is washed out in some cases. A synthetic seismogram analysis shows that this feature is caused by pP because it appears when the pP ray is added in (Burdick et al., 1984). Synthetics are shown at the bottom where it is also illustrated that the variation in the clarity of the feature could be due to a reasonable level of variation in the level of attenuation. It could also be associated with azimuthal variation in pP strength.

The implicit suggestion from these three figures that there is a close correlation between teleseismic short period P and regional P_n waveforms is a significant one. It implies that studies of the P_n waveform might be as fruitful as studies of teleseismic short period P have been for both discrimination and yield estimation purposes. The fundamental teleseismic discriminant, m_b - M_S, relies in part on short period P. A related discriminant might be built around the first few swings of P_n since that seems
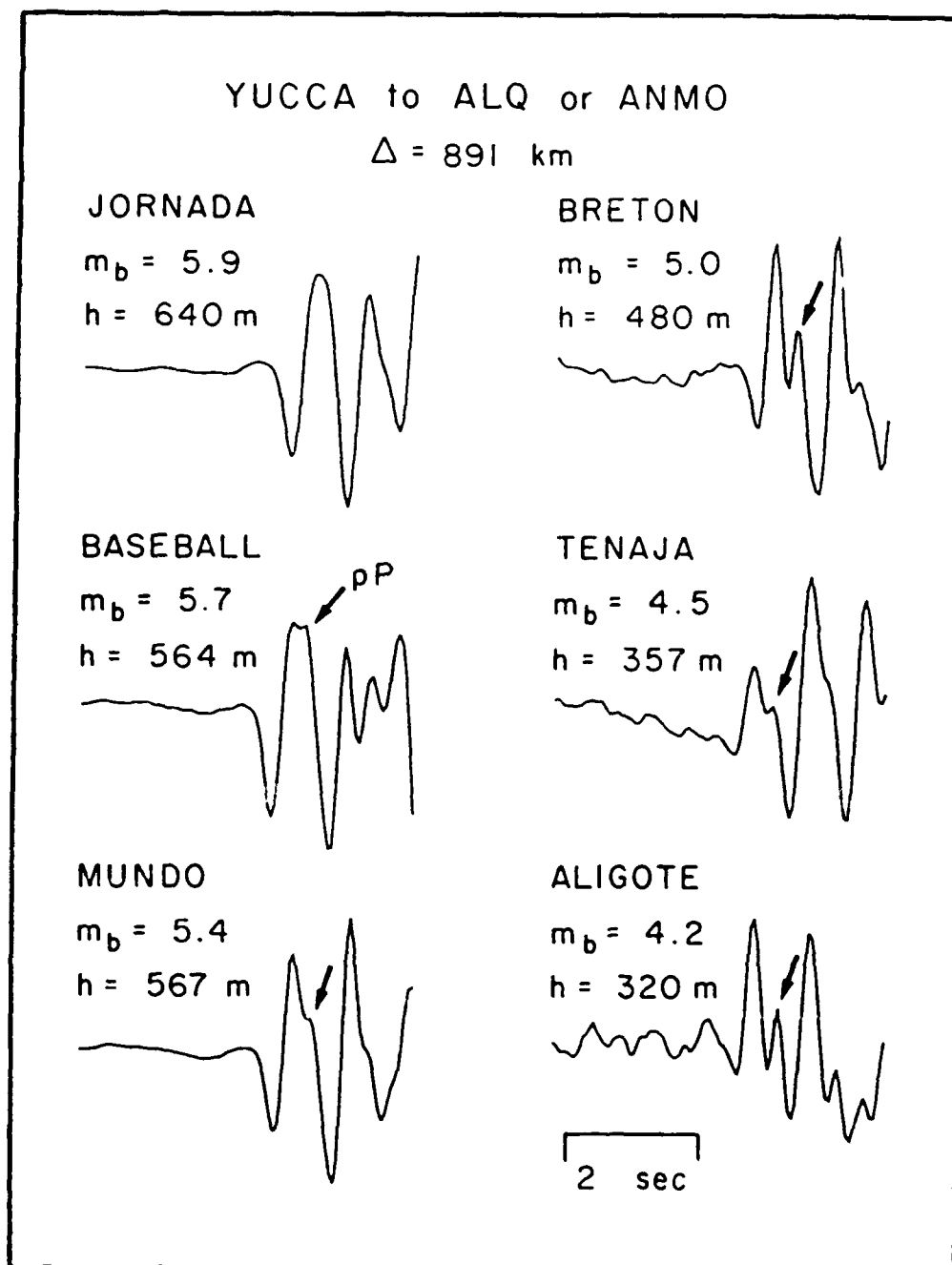
4

YUCCA to ALQ or ANMO

$\Delta = 891$ km

JORNADA

$m_b = 5.9$

$h = 640$ m

BRETON

$m_b = 5.0$

$h = 480$ m

BASEBALL

$m_b = 5.7$

$h = 564$ m

pP

TENAJA

$m_b = 4.5$

$h = 357$ m

MUNDO

$m_b = 5.4$

$h = 567$ m

ALIGOTE

$m_b = 4.2$

$h = 320$ m

2 sec

Figure 1. Observed P_n signals from Yucca events at DWWSSN station ALQ. The split "c" swing is interpreted as the effect of pP_n. As events get larger, the increase in the duration of the source function washes out the pP effect.
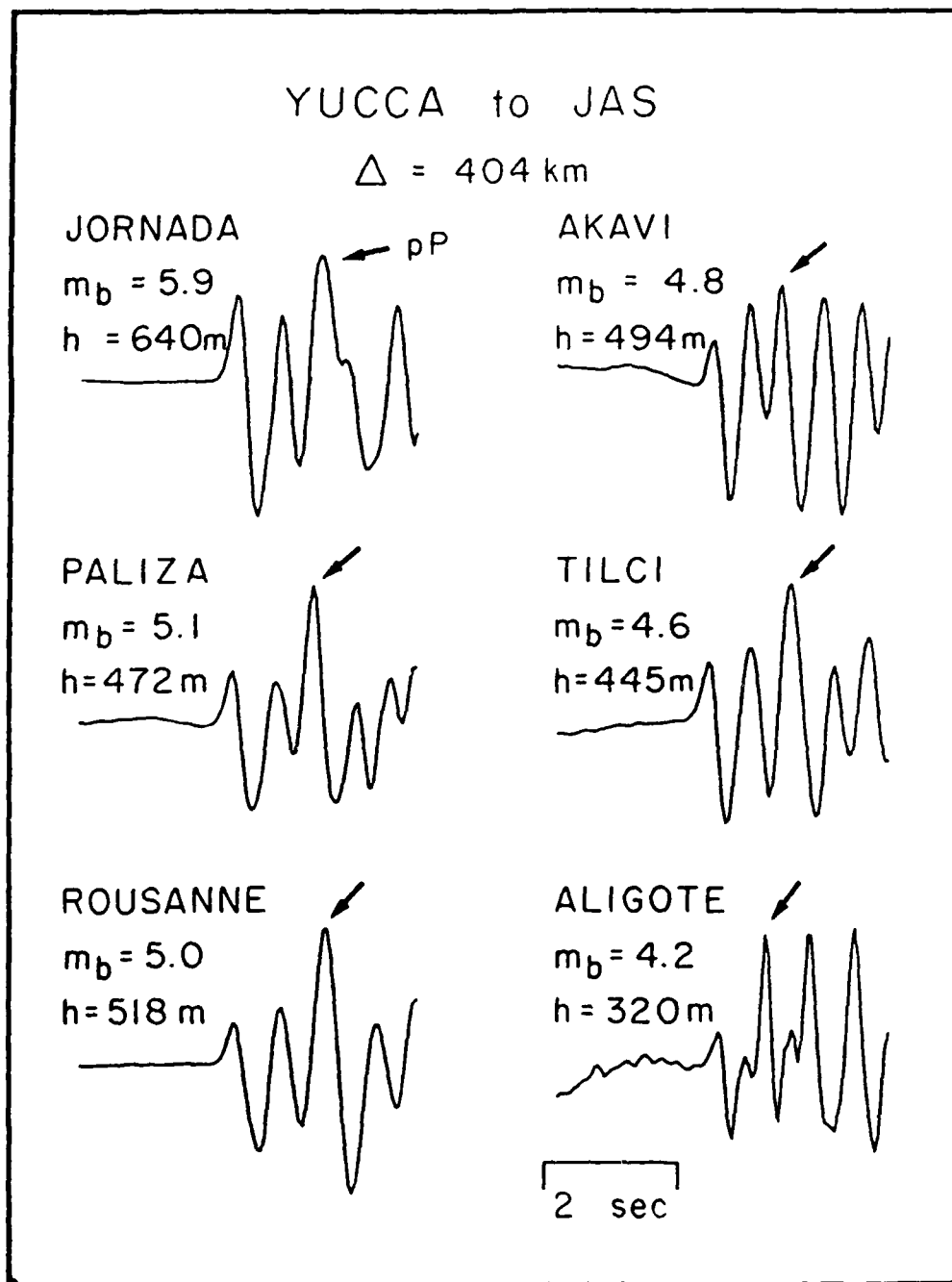
5

Figure 2. Observed P_n signals from Yucca events at DWWSSN station JAS. There is a correspondence in the evolution of the JORNADA and ALIGOTE signals in Figures 1 and 2.
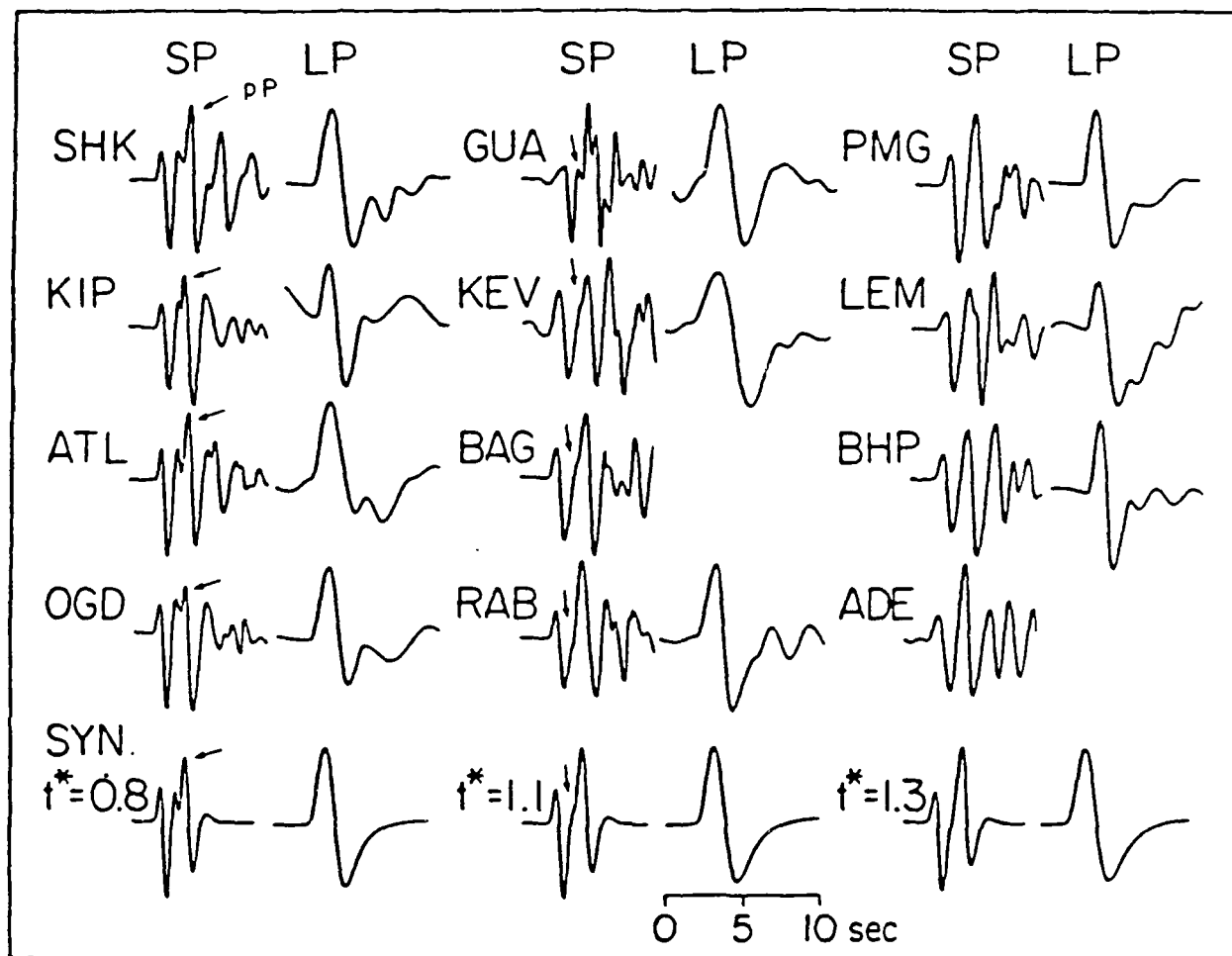
Figure 3. The teleseismic pP arrival can be observed as a distinctive double
peak in the "c" swing of some short period records from CANNIKIN. This is a
comparison of observed short and long period P waves with synthetics for a
range of t* values. As t* increases, the interference in the second upswing
produced by pP becomes less apparent. The synthetics were computed with an
artificially delayed pP.

to be a stable quantity. There are still many outstanding problems in the area of yield estimation and the understanding of explosion source physics. The most successful previous seismic studies of these problems have involved analysis of either near field or teleseismic data. There is difficulty in connecting these results because the teleseismic P waves are attenuated at an unknown and frequency dependent rate as they travel through the low velocity zone. The P_n waveform is not similarly affected. It can thus be used to test scaling laws, search for the effects of spall, test models for Q, and a number of other significant studies. It is interesting to compare the signals from JORNADA and ALIGOTE, the largest and smallest events in Figures 1 and 2. There is a clear evolution in frequency content between the signals, and since this evolution is so similar at the two stations, it must be source and not path related.

To ensure that this splitting of the "c" swing is not unique to the Yucca test site or the JAS and ALQ stations, we also examined P_n data from the Pahute test site and from the Yucca site at other stations. Figures 4 and 5 show that the P_n waveform at ALQ and JAS for Pahute Mesa events is very similar to that observed for the Yucca events. Another source of easily obtainable data exists in the form of the analog WWSSN film chips. In reviewing this data, we found that usually the gain was too high to permit inspection of the regional P_n waveform for NTS explosions. However, whenever there was an exceptionally clear trace, some indication of a split "c" swing could be observed. Figure 6 shows some hand digitized traces from the analog station BKS for Yucca events. The pP feature is indicated by arrows. Figure 7 shows similar data for GSC. This data clearly shows that the beginning of
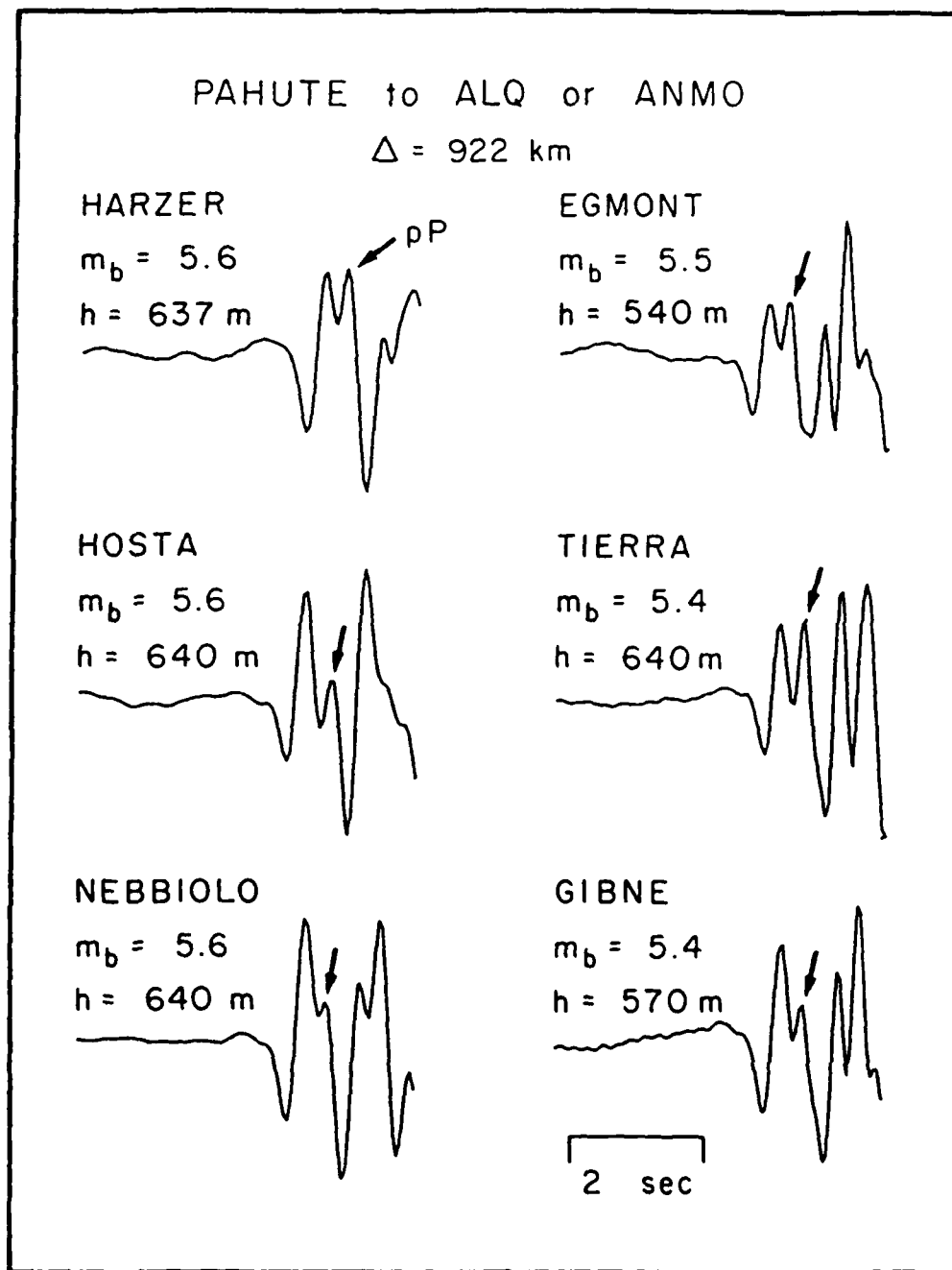
8

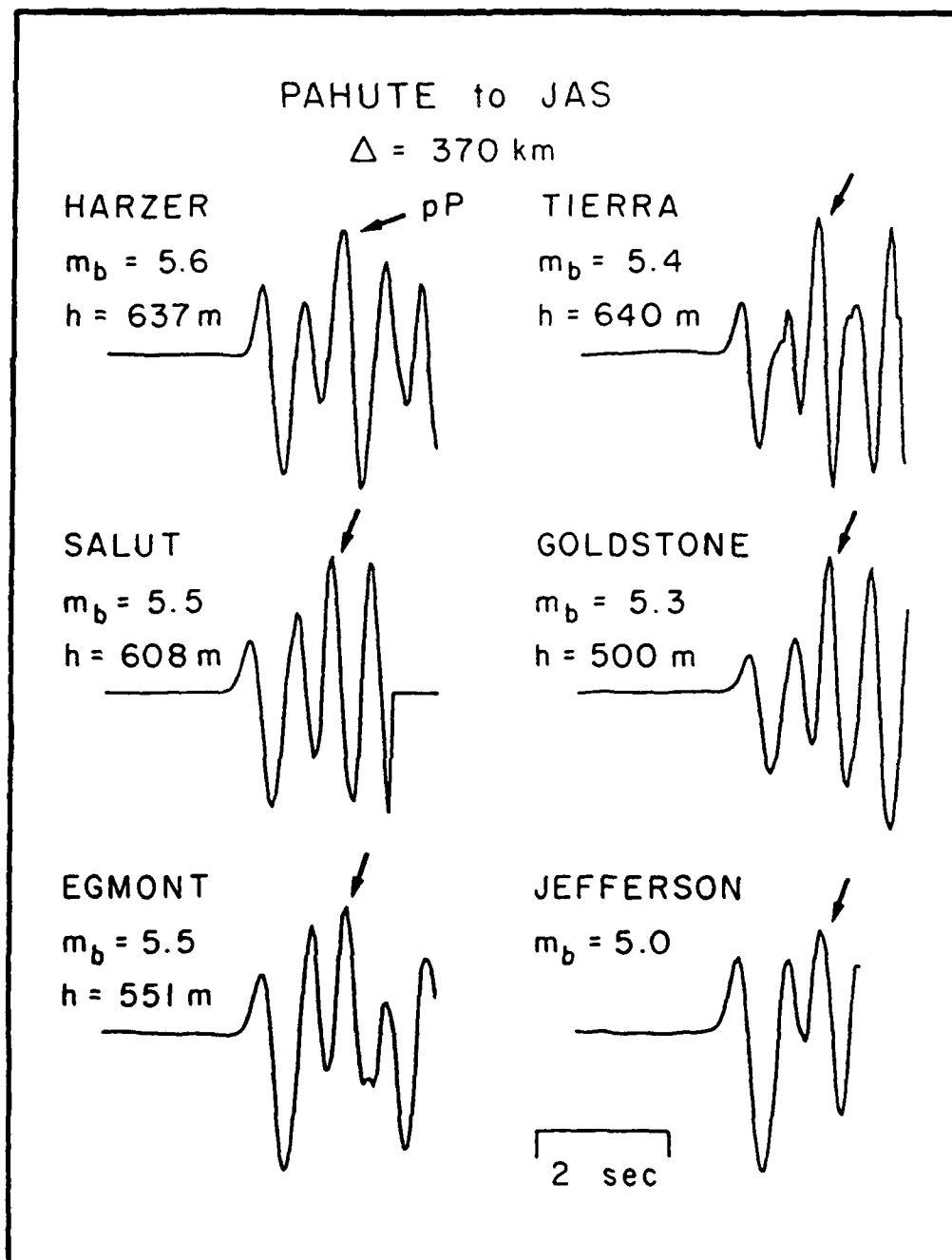Figure 4. Observed P_n signals from Pahute events at DWWSSN station ALQ. The split "c" swing is indicated by an arrow.

9

Figure 5. Observed P_n signals from Pahute events at DWWSSN station JAS. The split "c" swing is indicated by an arrow.
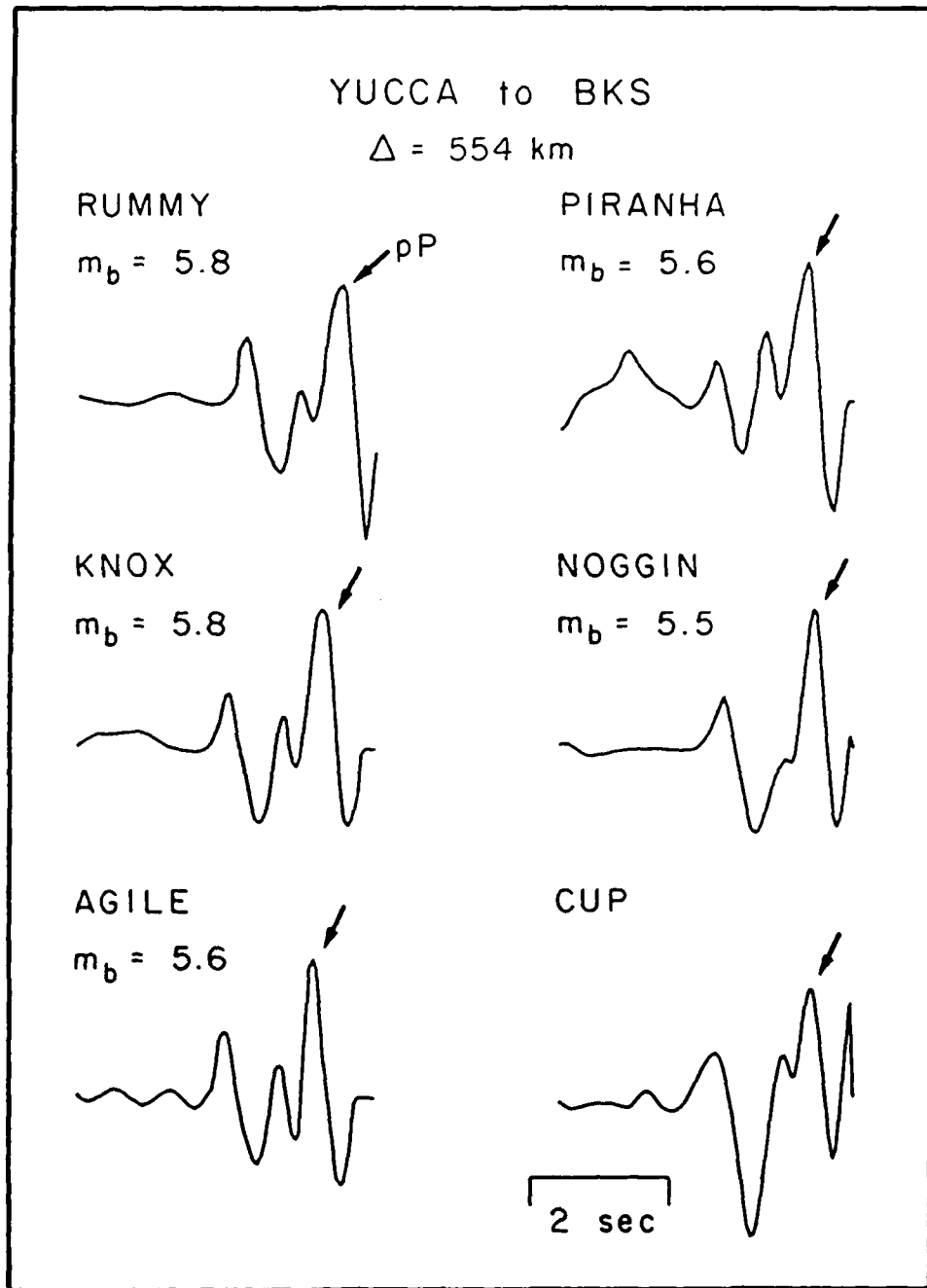
10

Figure 6. Observed P_n signals from Yucca events at WWSSN analog station BKS. The split "c" swing is indicated by an arrow.
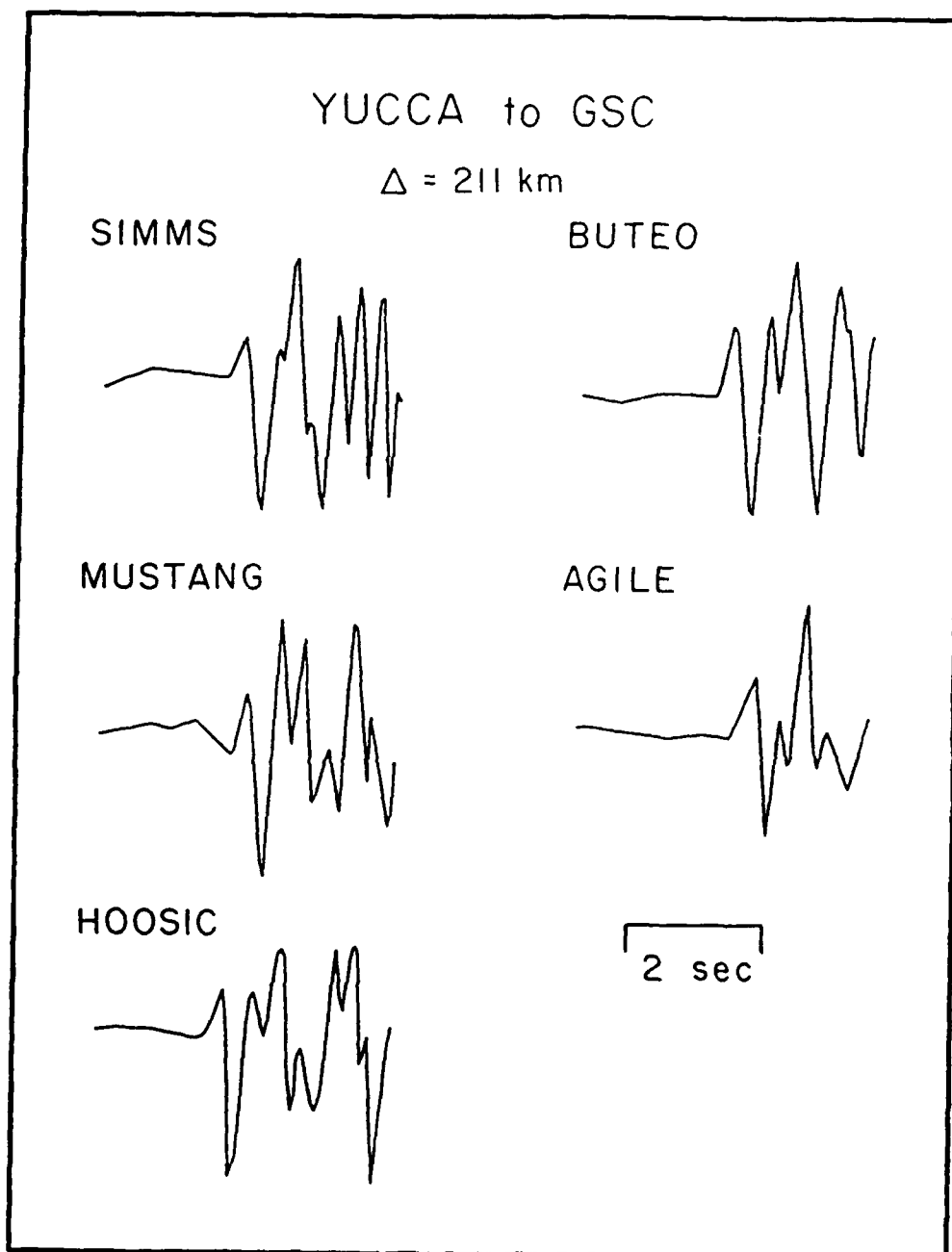
Figure 7. Observed P_n signals from Yucca events at WWSSN analog station GSC. The split "c" swing is indicated by an arrow.

12

the P_n waveform has a very stable character. If it can be shown that few earthquake P_n phases have this character, we have the basis of a short period regional discriminant.

The similarities between teleseismic short period P waveforms (Figure 3) and P_n waveforms would indicate that there is some similarity in the nature of the wave propagation. If this is true, then high frequency P_n should probably not be considered to be a true head wave, but rather a turning ray in the smooth gradient of the lid. To investigate the character of regional P_n in the western U. S. in more detail, we measured its speed at each of the four stations discussed above. The results are summarized in Figure 8. Time-distance plots are shown for each station along with a best fitting line and the apparent velocity. Wave speed does not increase monotonically with distance because the BKS speed is slower than the JAS. This only indicates, however, that velocity varies laterally in the lid. Furthermore, there is enough of a gradient in velocity (6.84 to 8.23 km/sec between 2 and 8 degrees) to support a strong turning ray. A similar increase in apparent velocity is associated with teleseismic rays spanning the ranges between 30 and 45°. It is therefore not unreasonable to suggest that P_n is a turning ray from the lid between 2 and 10°, at least in the western U. S.

For our initial calculations, we assume that the turning ray model for P_n is appropriate. We utilize the same methodology and assumptions used for computing teleseismic short period P. The response of the earth is assumed to be a delta function with an amplitude controlled by geometric spreading with the exception of the effects of near source structure. To simulate this effect, we use a plane wave calculation performed using propagator matrices.
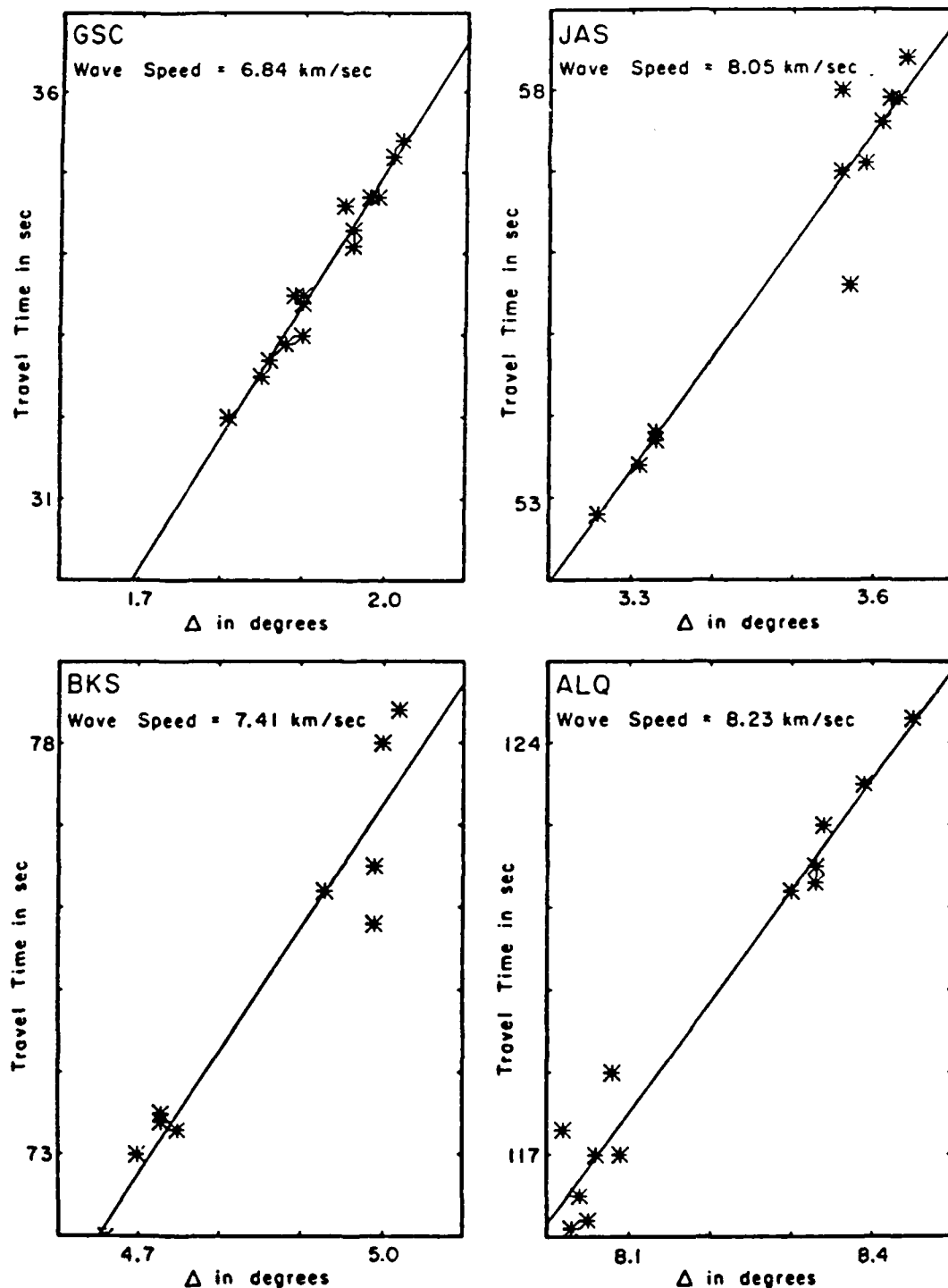
Figure 8. Determinations of wave speed of P_n at regional stations around NTS. Such information would be routinely available from an intelligent array and could be used in a discrimination algorithm.

14

We assumed a near source crustal structure based on modeling of near field data (Hartzell et al., 1983), and used a Pahute scaled Mueller-Murphy source. An apparent velocity of 8.3 km/sec was used which is appropriate for ALQ. The synthetics for four different source depths are compared to observed Pahute Mesa P_n phases in Figure 9. The observed feature in the "c" swing of the data is notably later in the observations than the synthetics, but the match of the bottom traces is actually quite good. The observation that actual pP arrival time is later than one would expect from elastic predictions has been made commonly (Burdick et al., 1984a,b) and is generally interpreted to mean that the arrival is a combination of elastic and inelastic effects over the source. Although we refer to the feature as pP here we acknowledge that it is probably something more complex. The key point, however, is that it is a depth related phenomenon and something thus could cause the basis for a discriminant. A correction for attenuation was initially included in the calculations. However, we found that the periodicity of the data was best matched for vanishingly small t^*. Q for P_n is apparently very high in the western U. S.

As was noted earlier, the "a" swing at ALQ is unusually broad and low in relative amplitude. We indicate the beginning of the "a" swing with an arrow in Figure 9. If P_n behaves as a true head wave, it should begin more gradually than if it were a turning ray. Thus, we may be observing some indication that this is the case at ALQ. At high frequency, an idealized head wave can be well approximated as the integral of the turning ray. We compare integrated synthetics to the ALQ observations in Figure 10. The smoothing effect can be seen in the differences between Figures 9 and 10, but the extreme smoothing of just the "a" swing is not matched. The pP feature begins to emerge, but not as strongly as for the turning ray case. It presumably
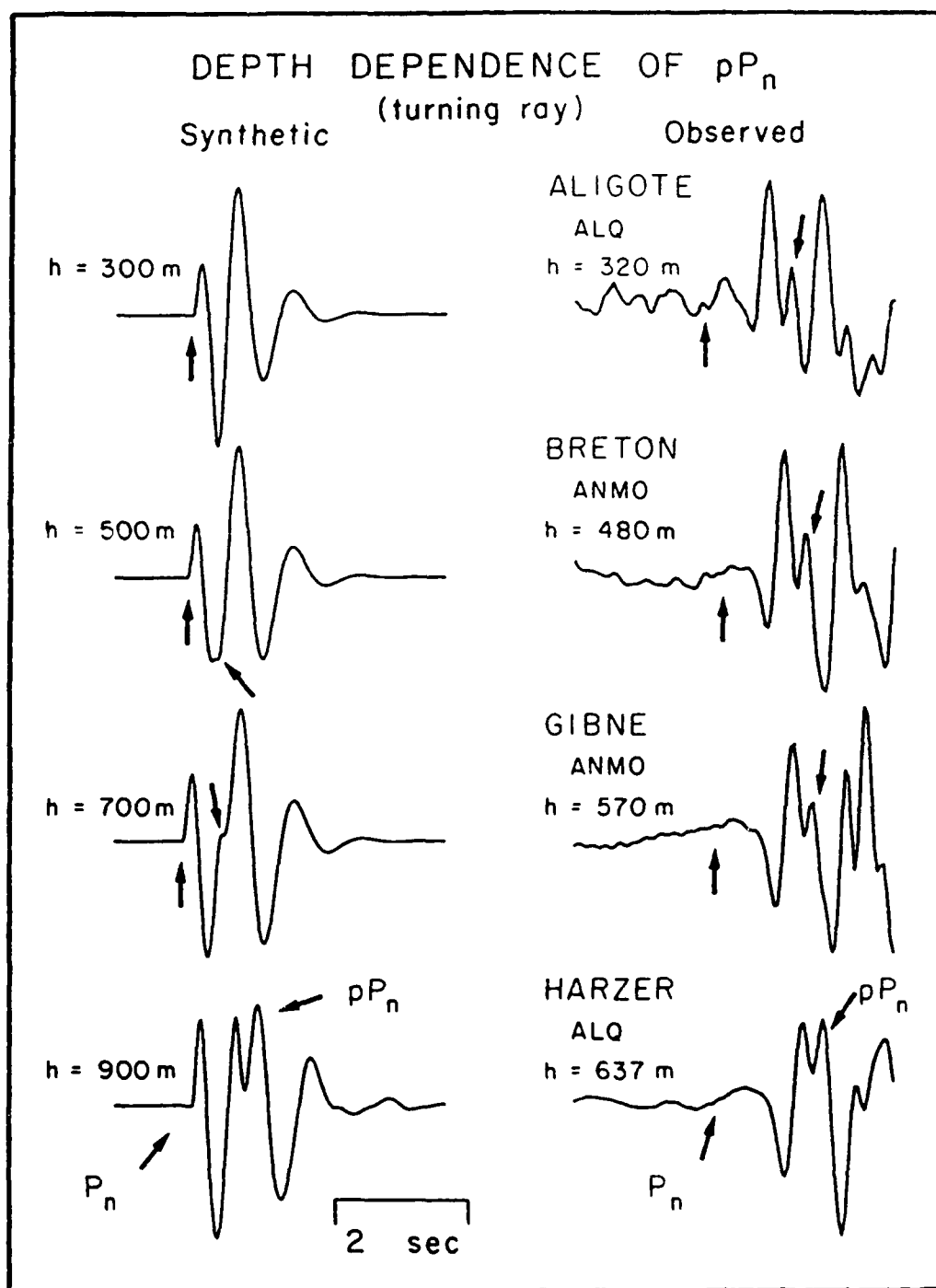
Figure 9. A comparison of synthetic to observed ALQ records from NTS explosions. We assume that P_n is a simple turning ray in the lid and perform a plane wave calculation using a structure for Pahute Mesa. The effective pP is obviously late.
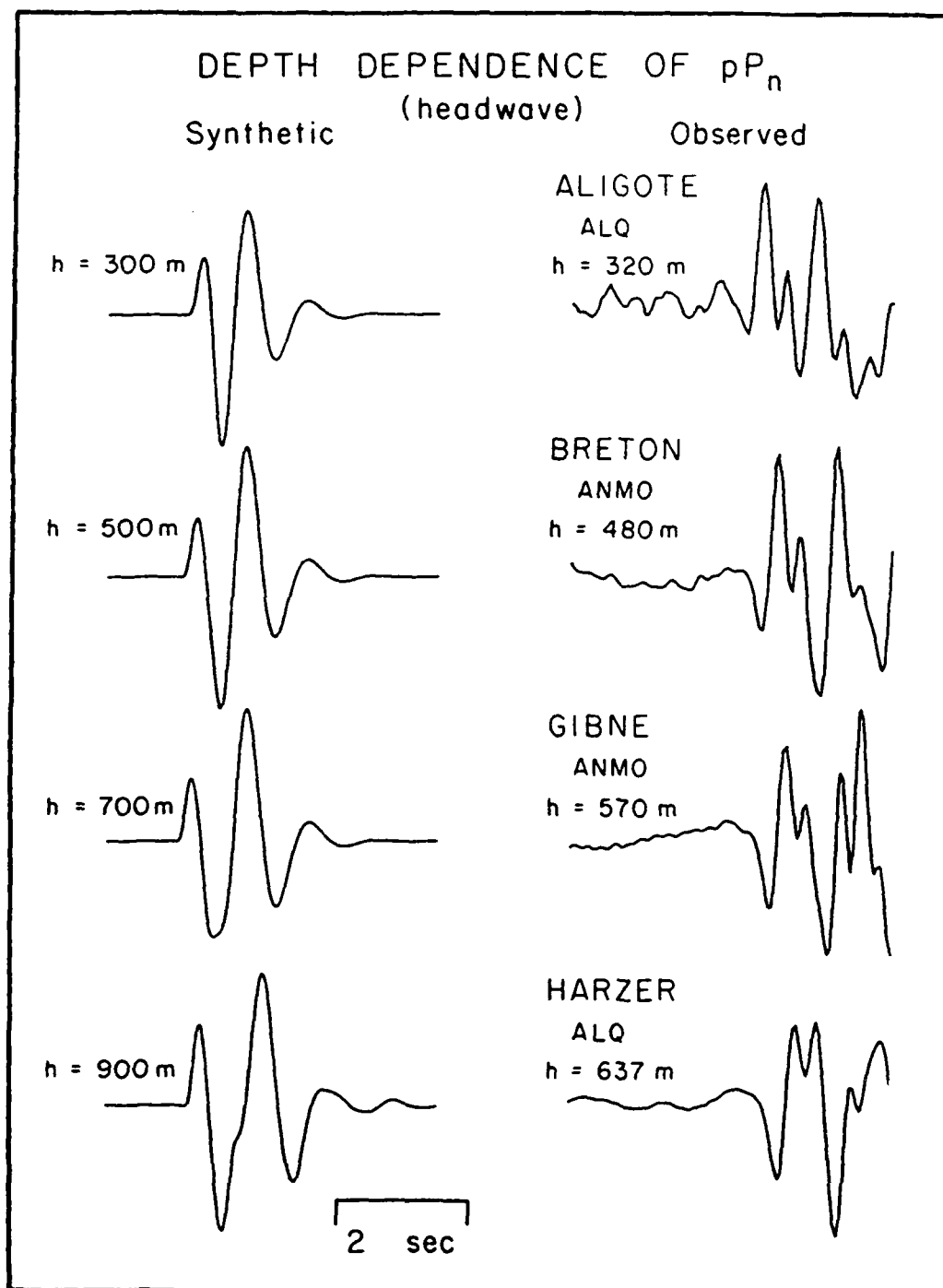
16

Figure 10. A comparison of synthetic to observed ALQ record from NTS explosions. We assume that P_n is a true headwave and through the wave front expansion

17

would for a deep enough depth, but the synthetics are already too long in period to match the data for the deepest depth shown. We believe that the representation of high frequency P_n as a turning ray is more appropriate. The unusual behavior at ALQ is more likely related to lateral variations in structure or to the frequency dependence of Q. In the latter case, we could be seeing some form of dispersion where the highest frequency energy arrives measurably ahead of the rest causing a precursor.

Averaging P_n: We have shown in previous figures that there can be little doubt that the splitting of the "c" swing by pP is a fairly general occurrence. There are, however, variations in the waveshape at each station. Some appear to be systematically related to event size and others to random scattering. In this section, we utilize each station as an array to stack for the average properties of the wave shape. The results of the averaging for the four stations are shown in Figures 11 and 12. The traces have been aligned to preserve the splitting of the "c" swing. The average P_n phases are shown together in Figure 13. The pulse shapes are most similar at GSC and BKS. JAS seems to have a much more deeply split "c" swing, but it otherwise correlates well with BKS. The pP feature appears to arrive earlier in the record from the most distant station, ALQ, as one should expect to see. It is interesting to note that the average P_n waveform does not change at a fixed station for the two different test sites. The average P_n waveform at JAS and ALQ is the same for Yucca and Pahute even though the test sites are more than 50 km apart. This implies that the average P_n waveforms at the stations are stable and not strongly affected by near source structure. This is an important fact because the ability to discriminate based on this pP phenomenon will depend strongly on how well the waveform for a new source-site
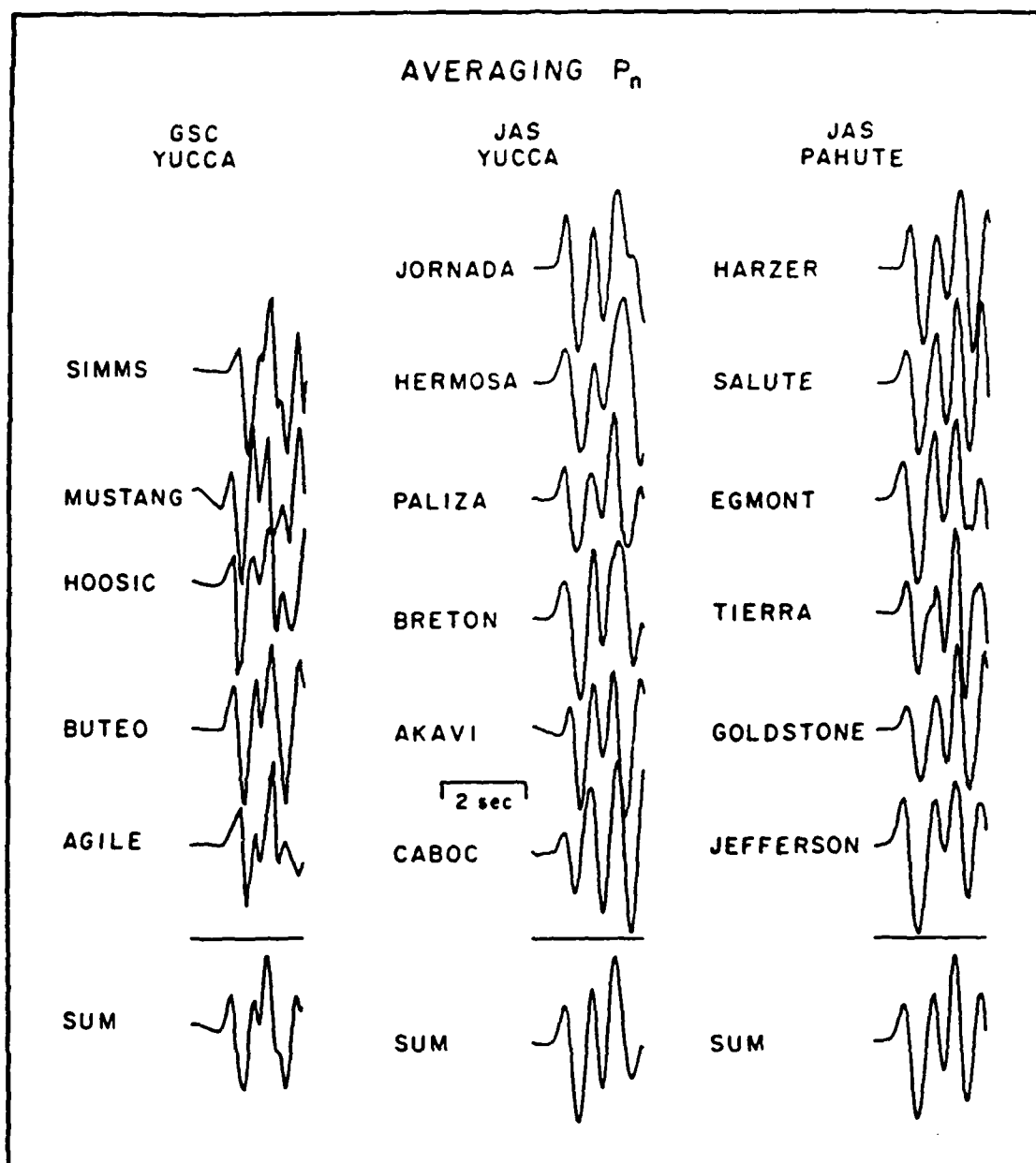
18

Figure 11. The average P_n waveshape at GSC and JAS is relatively consistent and displays the split "c" swing. The sum of the individual traces is shown at the bottom.
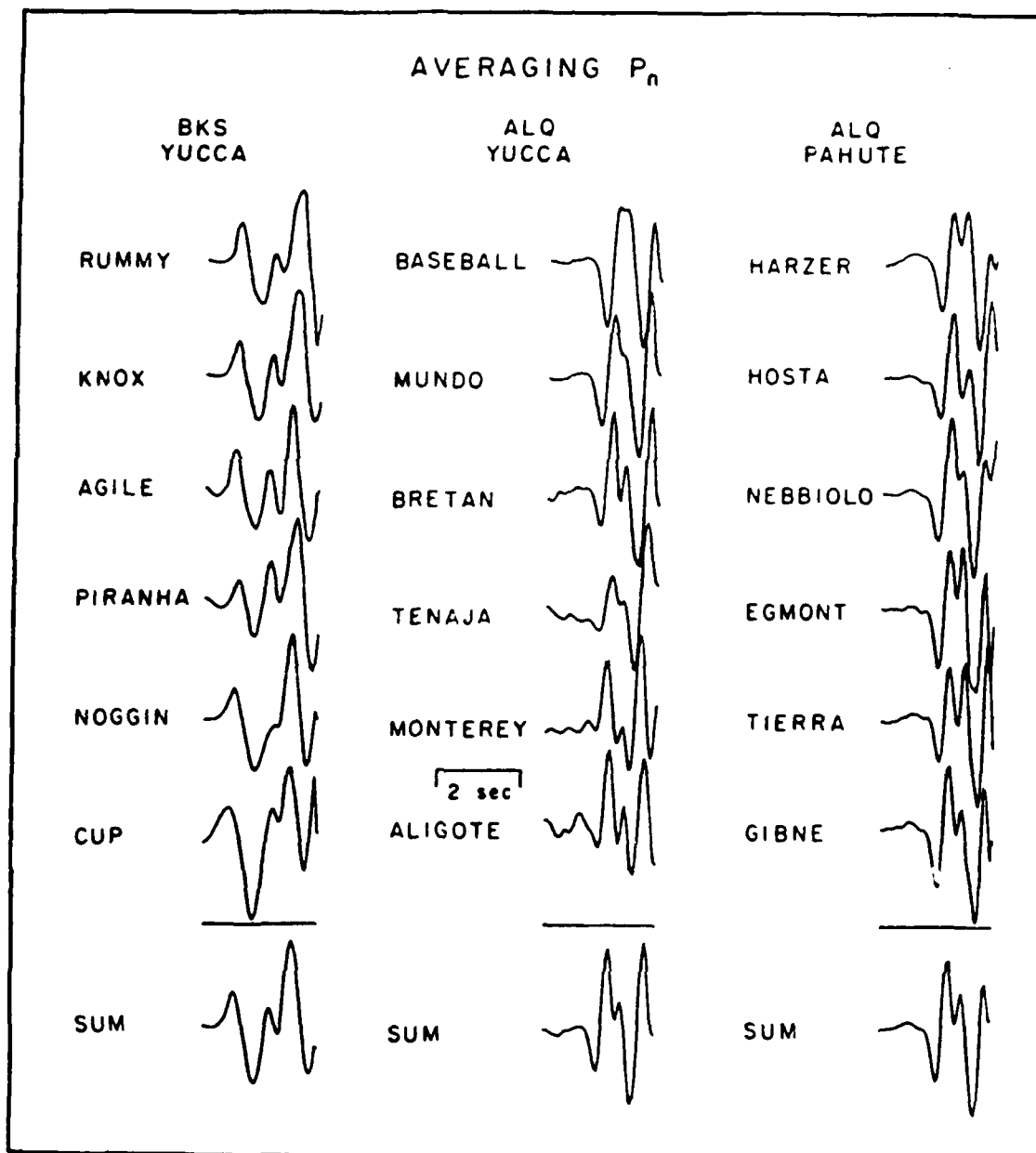
Figure 12. The average P_n waveshape at BKS and ALQ is relatively consistent and displays the split "c" swing. The sum of the individual traces is shown at the bottom.
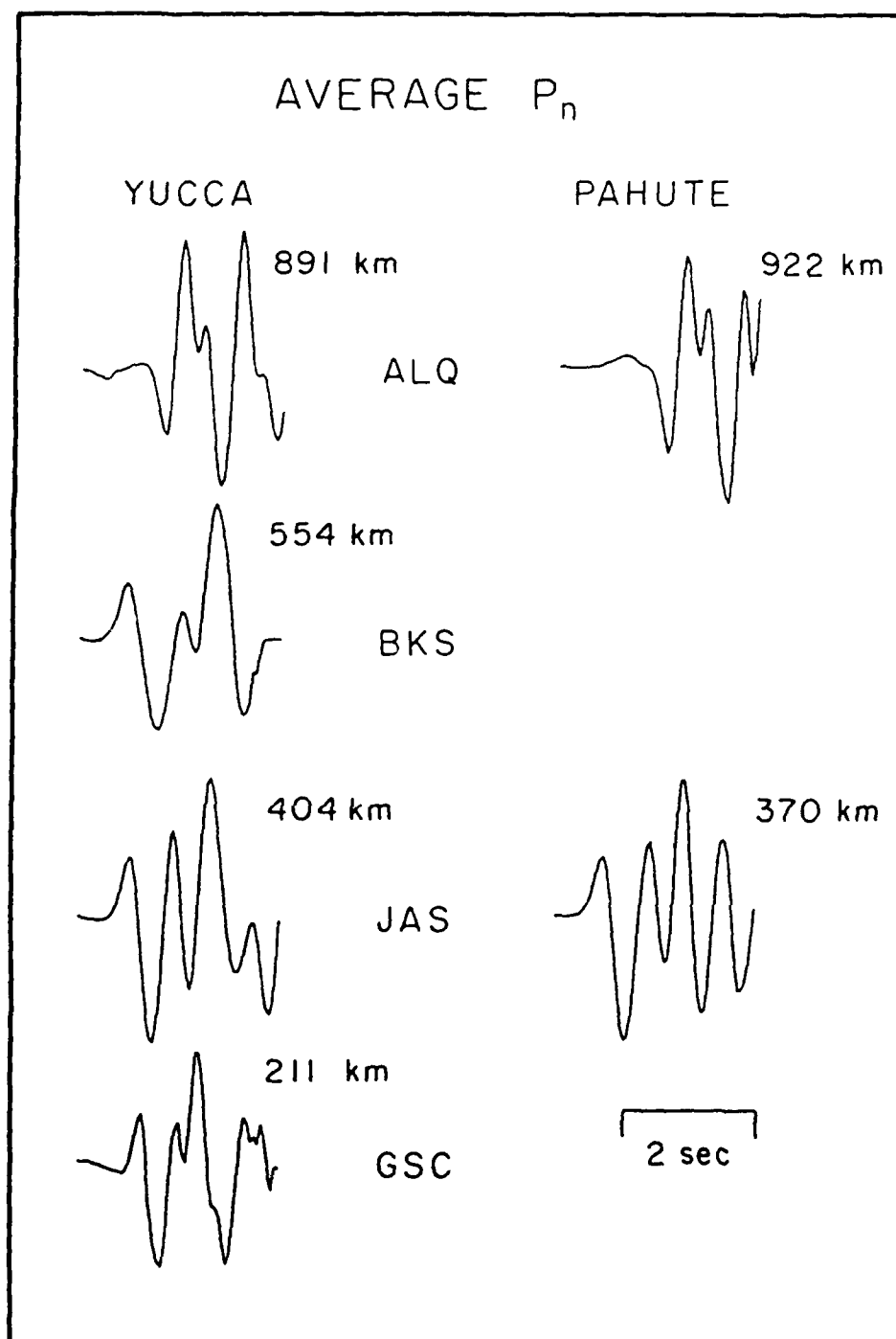
Figure 13. A summary of the average P_n's regional from stations around NTS. The average P_n does not vary at a given station between Pahute and Yucca.

combination can be predicted. The conclusion of this exercise is that the pP interference is a pervasive feature, and insofar as it really is caused by the free surface, one should expect to see it for any contained test. The next question which must be answered is how often similar features appear in earthquake waveforms.

Discrimination using P_n: To address this question, we assembled a data base of 31 observations of western United States earthquakes from stations ALQ and JAS. The earthquakes were selected to be as close to NTS as possible, but to obtain enough samples we needed to accept events from as far away as southern California. We estimated the P_n arrival time as accurately as we could and windowed out the first three seconds of the arrival. Representative samples which were selected at random are shown in Figures 14 and 15. We compared these signals to the average explosion P_n waveforms shown in Figure 12 using the analytic norm introduced by Burdick and Mellman (1976). This norm increases uniquely to a value of one if and only if two signals are identical. It can be shown to be closely related to the L2 norm for two traces if they are aligned at the time of maximum correlation (Burdick, 1985).

The results for Pahute events at JAS are shown in Figure 16. The separation of the explosion and earthquake populations is complete indicating that the beginning of an earthquake signal is systematically different from the beginning of an explosion signal. The results for Pahute events at ALQ are shown in Figure 17. Again the discrimination between events is quite good. Unfortunately, most events from Pahute Mesa are relatively large. The discrimination shown in Figures 16 and 17 is not in the small ($m_b < 4.0$) magnitude range where discrimination is difficult using standard techniques.

22
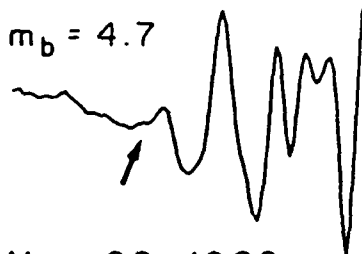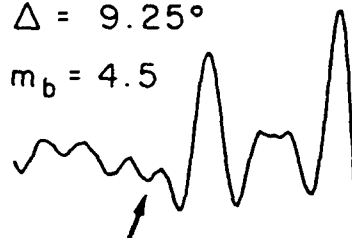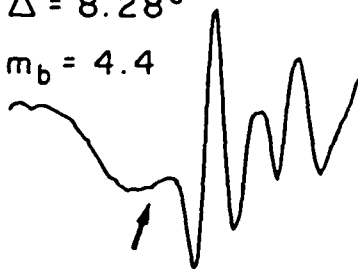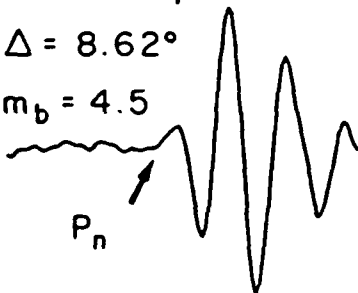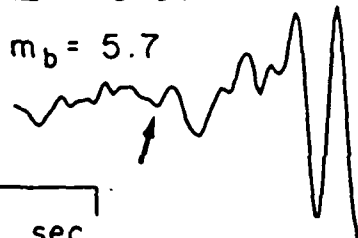
Figure 14. A data base of digital P_n arrivals from western U. S. earthquakes has been assembled from station ALQ. These are the first 6 arrivals chosen.
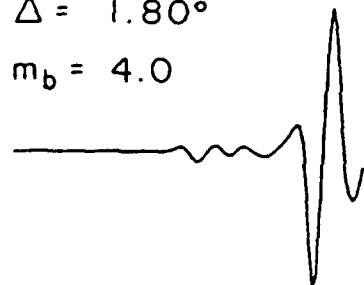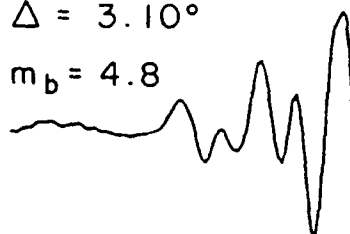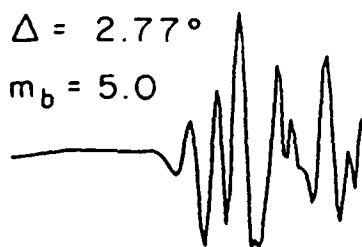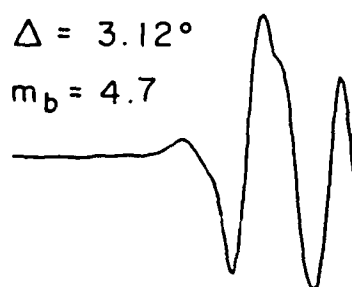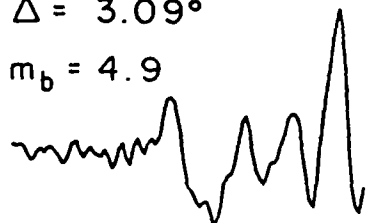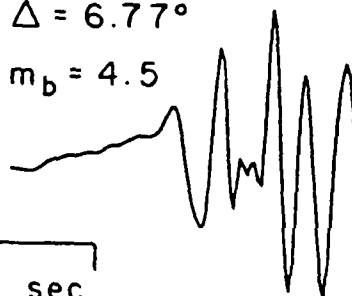
Figure 15. A data base of digital P_n arrivals from western U. S. earthquakes has been assembled from station JAS. These are the first 6 arrivals chosen.

24

Figure 16. Discrimination of Pahute explosions from earthquakes using the correlation with the average P_n waveform at JAS. The explosions are stars and the earthquakes squares.

Figure 17. Discrimination of Pahute explosions from earthquakes using the correlation with the average P_n waveform at ALQ. The explosions are stars and the earthquakes squares.

Smaller events are generally located at Yucca Flat. The results for Yucca events at JAS are shown in Figure 18. The stars were generated using the P_n waveform shown in Figure 11. The separation is again good above magnitude 5 but definitely begins to deteriorate as magnitude decreases to 3. The smallest explosion in the data set is PINEAU (m_b ~ 3.3), and its correlation with the average explosion P_n is comparable to that of earthquakes. Nonetheless, the P_n waveform does appear to have some discrimination power between magnitude 3 and 4 where new discriminants are needed.

Part of the deterioration of the discriminant at small magnitude is due to the fact that the average waveform used for the correlations came from larger events. We averaged the waveforms from 6 small explosions and correlated them with the earthquakes to produce the crosses in Figure 18. The event PINEAU is clearly separated from the earthquake population. The large explosions are not nearly as well correlated with this estimate of average P_n (i.e. the crosses are lower than the stars at large magnitude) indicating that there is a size effect which needs to be taken into account in using this discriminant.

Figure 19 shows the results for Yucca events at ALQ. Again the populations are separated, but discrimination power decreases with magnitude. We have examined some of the worst cases and find that this is primarily a signal to noise effect. It is important to note that if we were working with array data like that from NORESS, we could process the signals to improve signal to noise. Moreover, it is well known that P_n amplitudes are generally much higher in stable continental areas than the western U. S., so we can
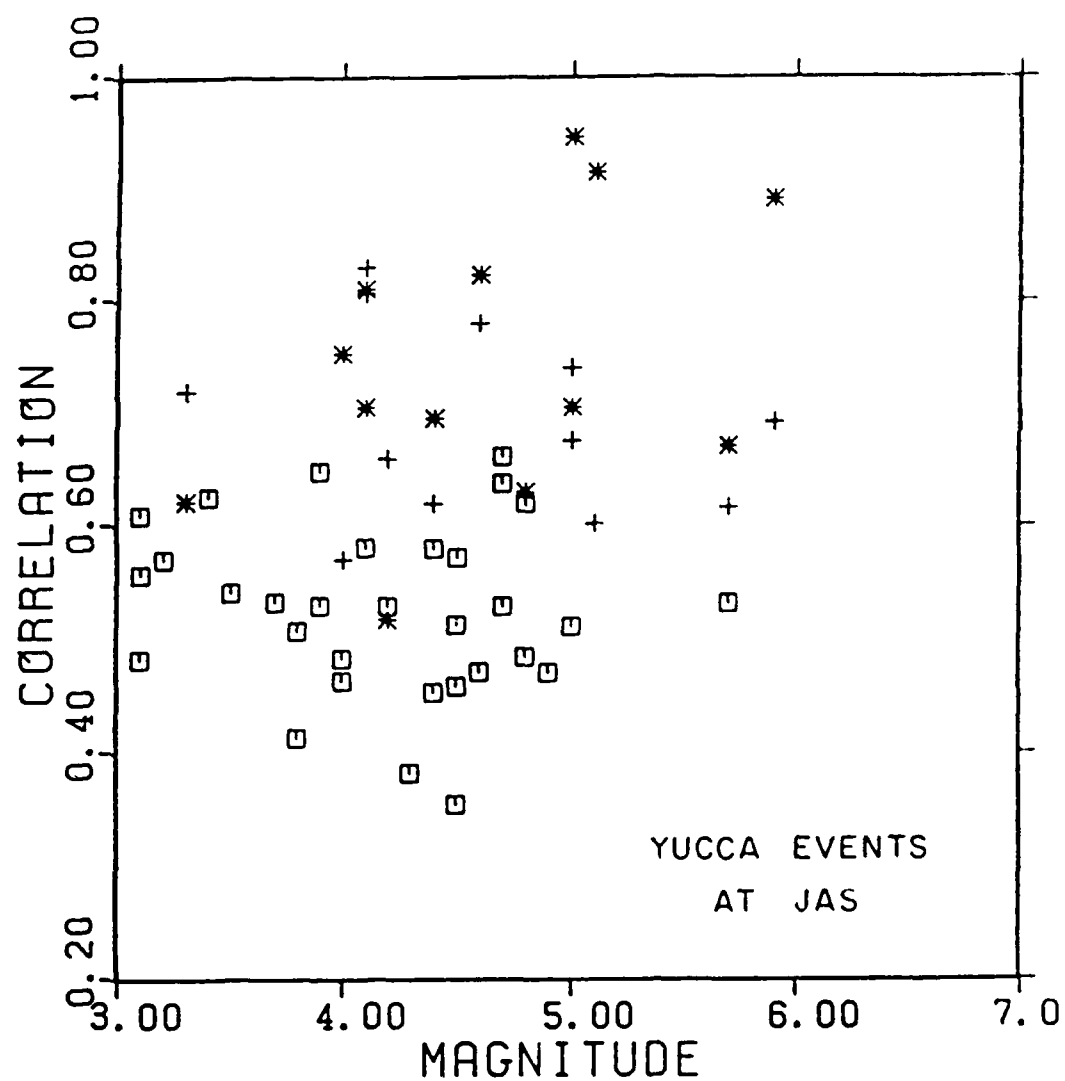
Figure 18. Discrimination of Yucca explosions from earthquakes using the correlation with the average P_n waveform at JAS. The explosions are stars and crosses and the earthquakes are squares and. The stars represent correlation with the average moderate event waveform and the crosses with the average small event.
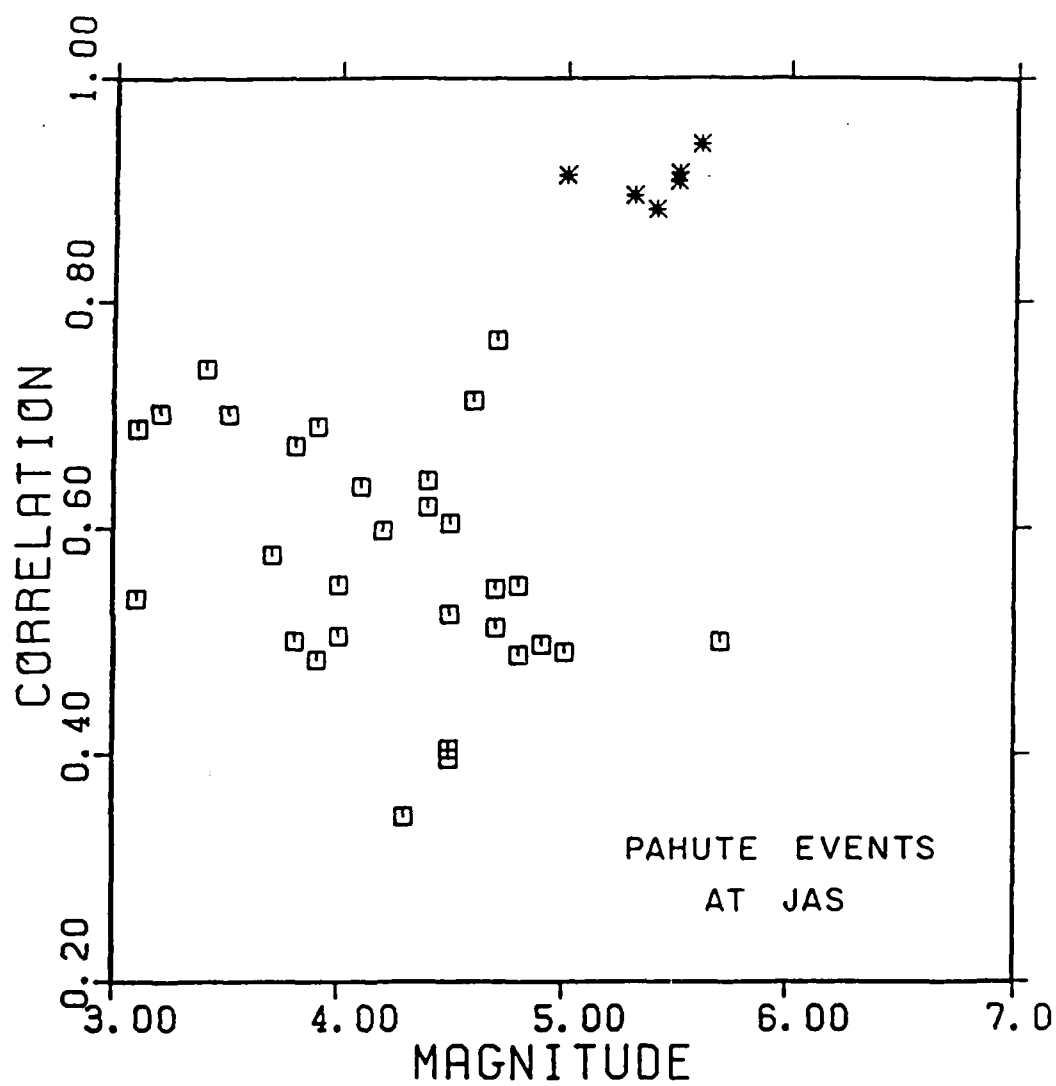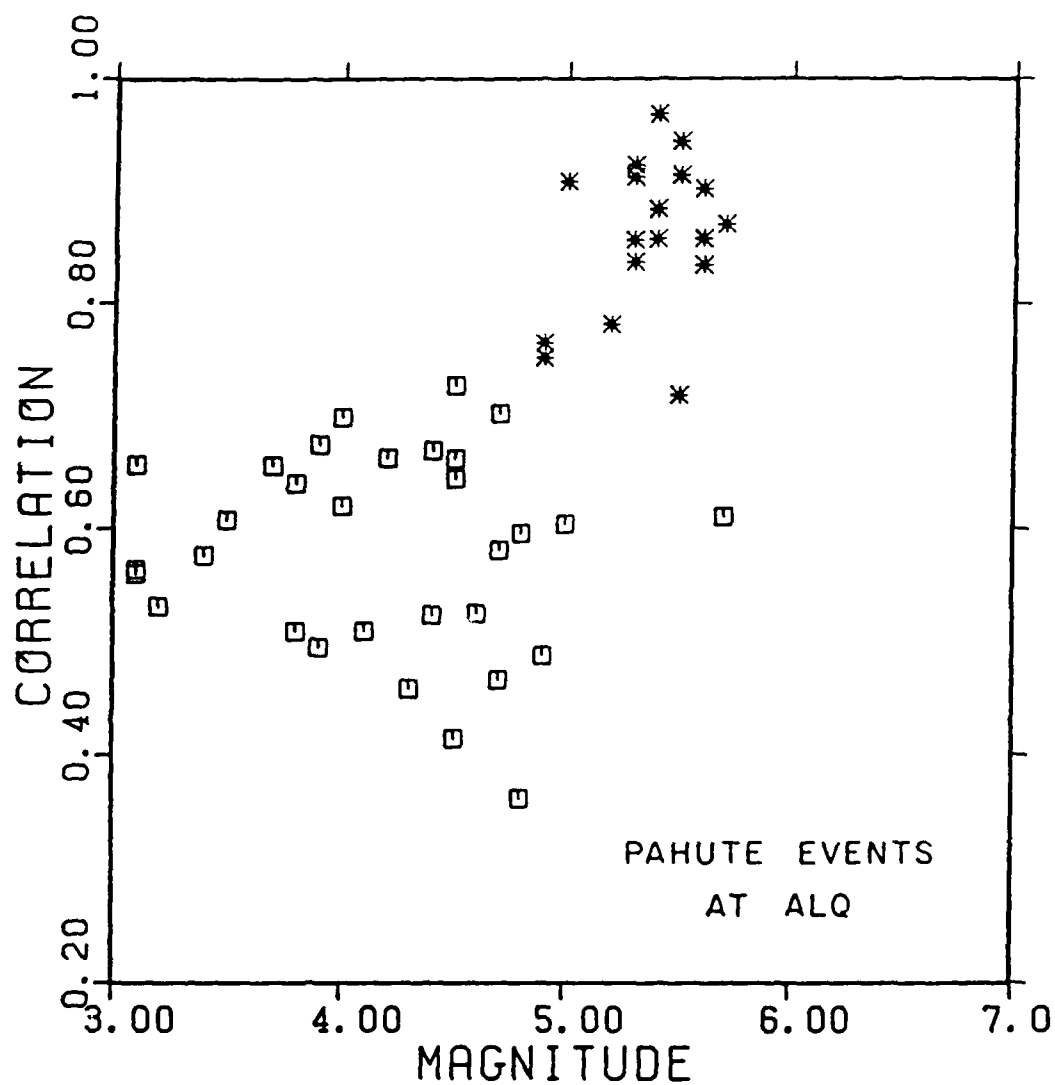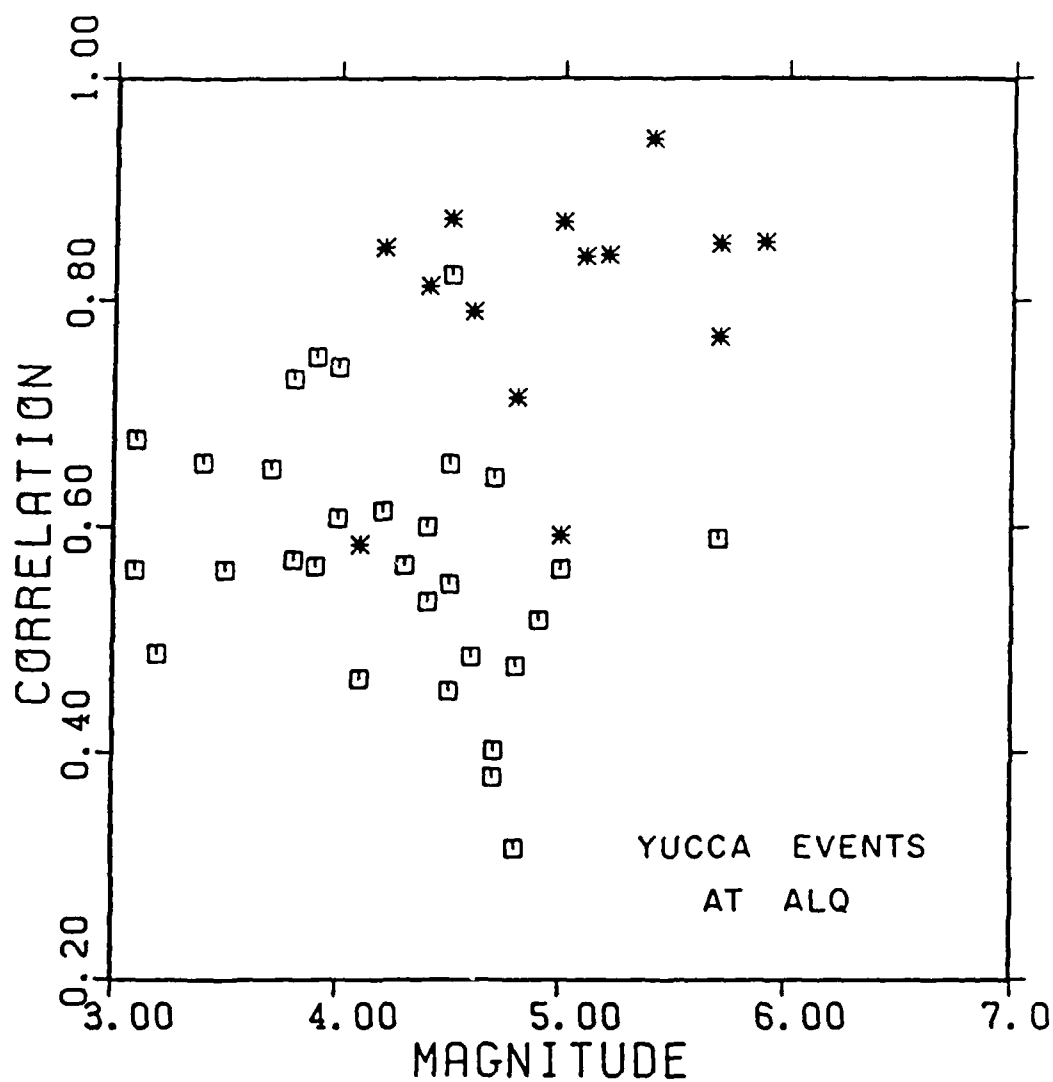
Figure 19. Discrimination of Yucca explosions from earthquakes using the correlation with the average P_n waveform at ALQ. The explosions are stars and the earthquakes are squares.

anticipate good signal to noise ratio down to magnitude 3 and less.

As a final exercise, we test the observation made earlier in Figure 13 that there does not seem to be much variation in average P_n waveform between the two test sites at a fixed station using the quantitative norm. In Figures 20 and 21, we show the correlation between all explosion waveforms and the average Yucca P_n waveform for ALQ and JAS respectively. There is effectively no separation of the two populations indicating that the average wave shape is not strongly dependent on near source structure. This is a result that is surprising at such high frequencies but welcome because it indicates that we may be able to develop a stable discriminant.

Such a discriminant could be based on a wide variety of underlying strategies and waveform comparators besides the one we have been using so far. The important result we have shown is just that the onset of P_n for explosions is stable and unique. One strategy for a discrimination procedure would be a purely empirical one. As large a data base of average P_n waveforms as possible could be assembled from U. S., Soviet and French test sites. This data base could then be compared continuously to the digital P_n signals as they stream into the global array. With modern processors, this operation could be done very rapidly for a large background data base of average P_n phases. The decision could continuously be made whether P_n signals from new events look like P_n phases observed from previous explosions. An alternate method could involve development of a synthetic predictor of P_n waveforms based on source to station distance, event magnitude, observed P_n wavespeed and other source parameters. A third approach could involve the new computer based recognition techniques highly tuned to the P_n waveform.

30
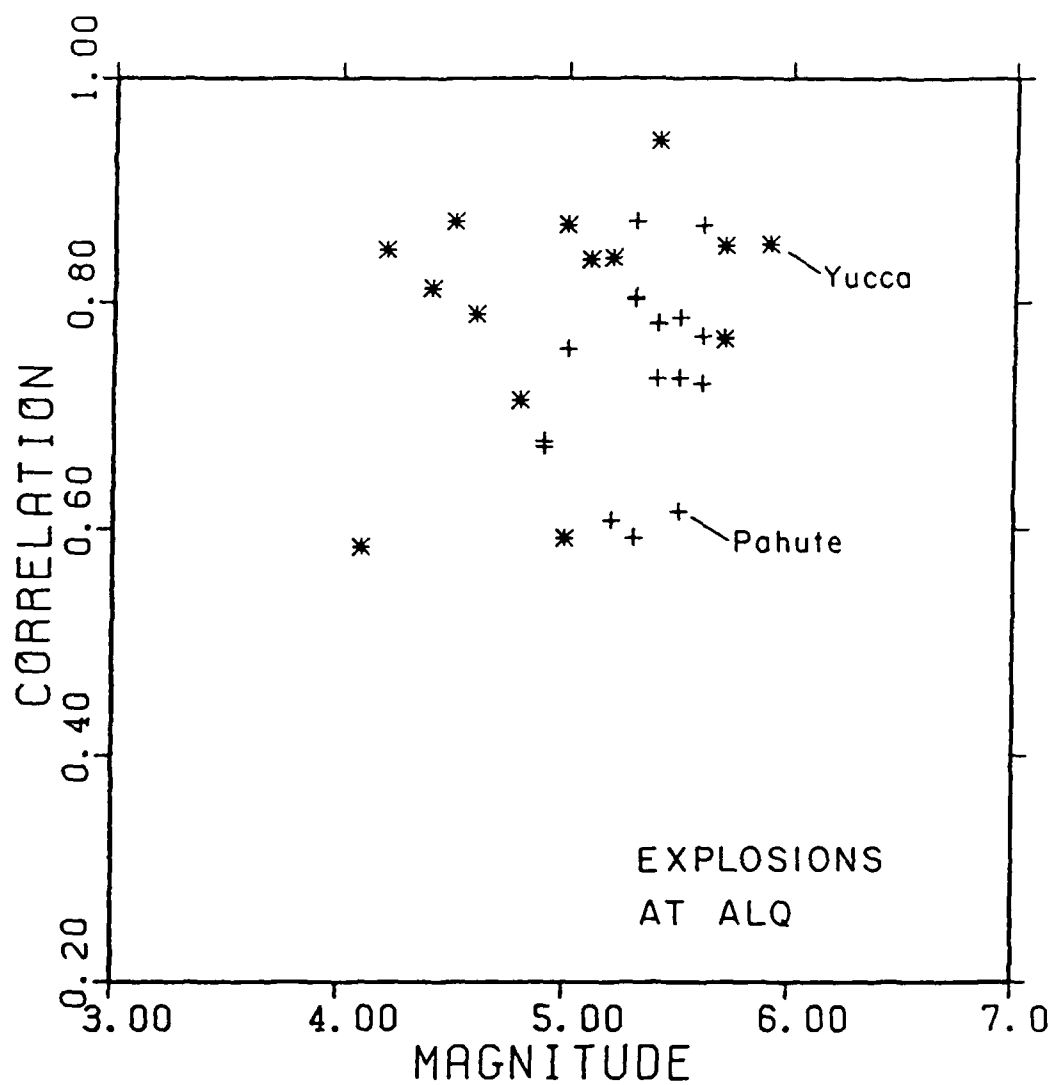
Figure 20. Correlation of P_n waveforms from either Pahute or Yucca events with the average explosion P_n waveform at ALQ.

31
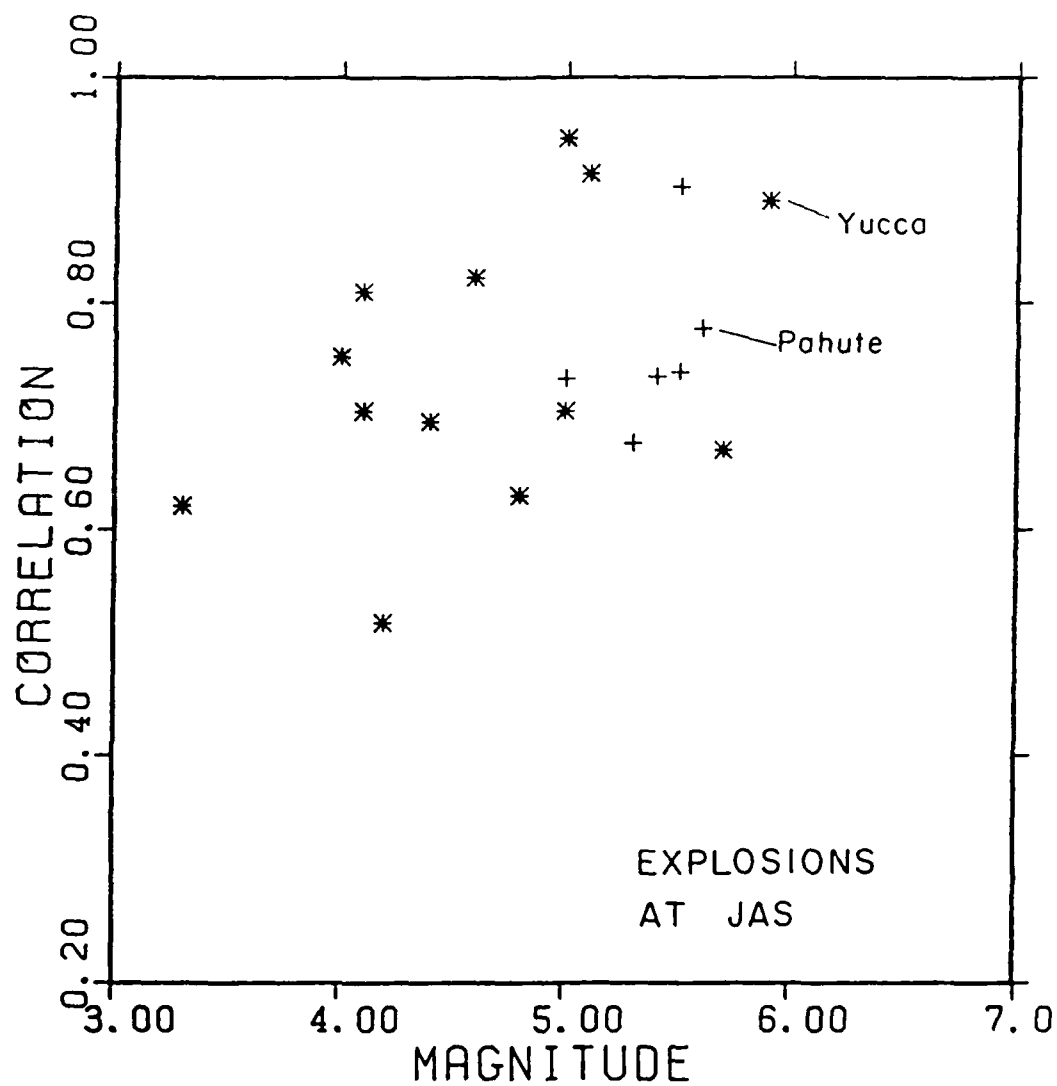
Figure 21. Correlation of P_n waveforms from either Pahute or Yucca events with the average explosion P_n waveform at JAS.

The Crustal Resonance Phase Discriminant

The chief drawback to using regional P_n as the basis for a discriminant is that it does not have as high an amplitude as other regional phases. Its advantage is that it is the first arrival on the record, and the idea of a waveform for it is meaningful as was demonstrated in the preceding section. In this section, we discuss an attempt to base a discriminant on some of the higher amplitude arrivals. The phase P_g was selected for study in this, the developmental phase of the project, where data from the western U. S. are being analyzed. The reason for making this selection is illustrated in Figure 22. A suite of digital regional waveforms from explosions and earthquakes are displayed in a seismic section. In terms of signal to noise ratio, the most effective discriminants should be based either on P_g or the S_g - Lg complex. We indicate the predicted moveout of PmP, S_n and SmS for an appropriate crustal model to illustrate two points. The first is that the P_n - S_n discriminant which was developed using NORESS data by Dysart and Pulli (1988) can not be tested in this tectonic environment. There is effectively no S_n in this frequency band. The second point is that the P_g and S_g wave complexes begin at PmP and SmS times respectively although they have a duration many times longer than could be explained by just these phases. The reason for the long duration of at least P_g and possibly S_g as well was discussed by Burdick and Helmberger (1988) who show that the complex is made up of a series of pulses called crustal resonance phases. They are built up by groups of rays reverberating in the crust. This sequence of pulses and their coda account for the character of P_g. Similar rays in the shear mode may account for S_g. The advantage of studies made in the time domain is that deterministic concepts seem to apply much better at times before coda builds up. It seems

33
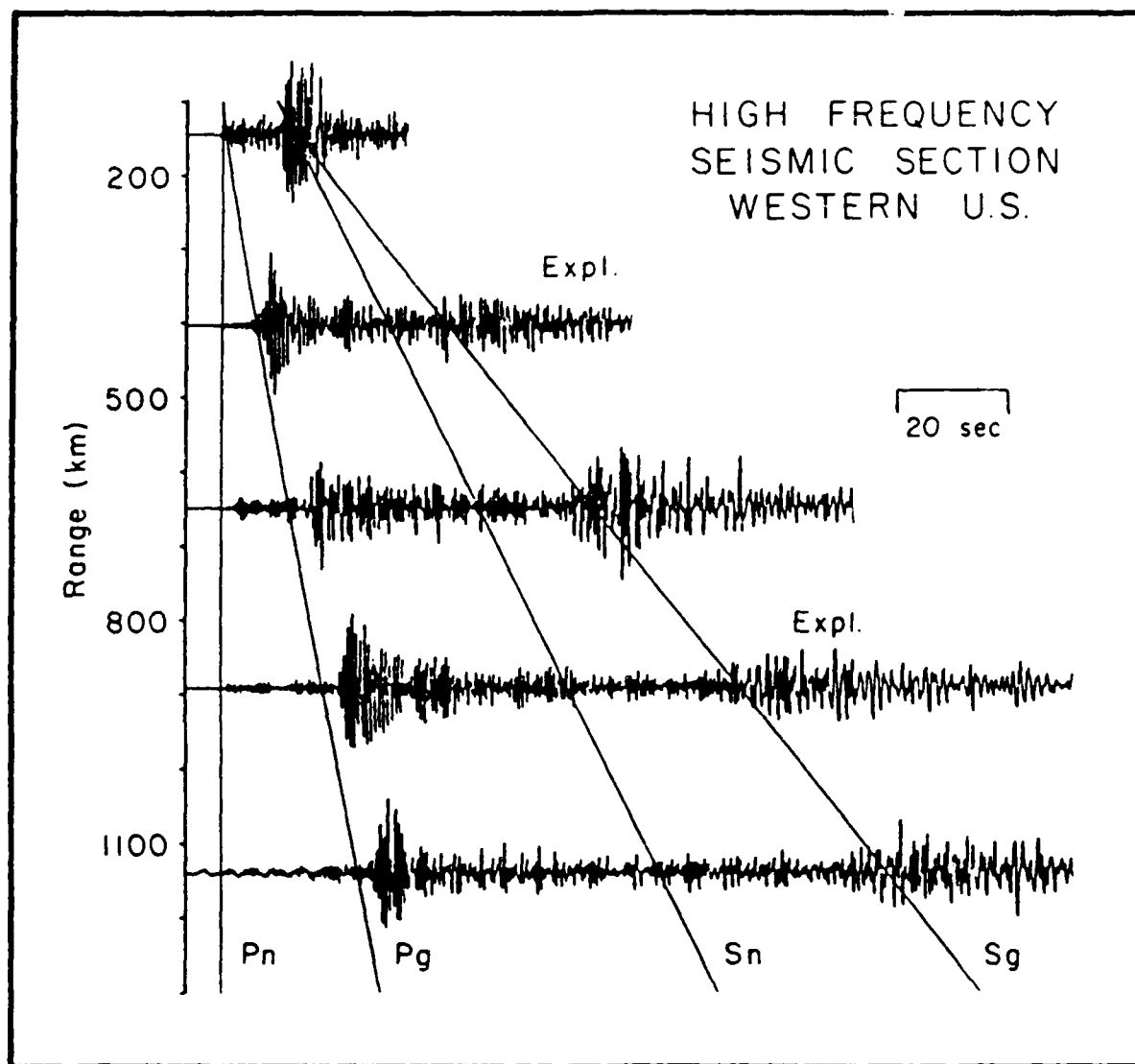
Figure 22. A short period seismic section of explosions and earthquakes for the western U. S. The P_g and S_g arrivals commence with PmP and SmP. There is no S_n arrival in this frequency band.

logical therefore to analyze the beginning of P_g to find any deterministic character on which a discriminant could be based since it is the first of the high amplitude regional arrivals and it generally overwhelms P_n.

There have been several deterministic modeling studies of the onset of P_g although they have not widely been recognized for what they are. This is because they have been performed on data in the long period band and are generally termed Pnl studies. Though the emphasis in these studies was on the long period energy, the forward synthetics often match the short period details of observed seismograms remarkably well. To illustrate the correspondence between P_g and the arrivals in the long period band, we show a section of long period records from NTS explosions in Figure 23 over a range comparable to that shown in Figure 22. The long period energy at the beginning of the records is made up of a complex of head waves and the shift to higher frequency is related to a complex of reflected rays. The correspondence of this reflected energy and P_g is obvious. The data in Figure 23 were the data used in a well known study by Wallace et al. (1983) to deterministically characterize the effects of tectonic release. We have also deterministically modeled it along with comparable western U. S. earthquake data as described in a previous report on this study (Burdick and Helmberger, 1988).

To further this phase of the work and to ensure that the results from the western U. S. will be applicable in other tectonic environments, we have examined Pnl waves from two eastern U. S. earthquakes recorded at eastern U.S. and Canadian stations. These were the 9/4/63 Baffin Bay earthquake and the 1/9/82 New Brunswick event. The results are shown in Figures 24 and 25. As

35
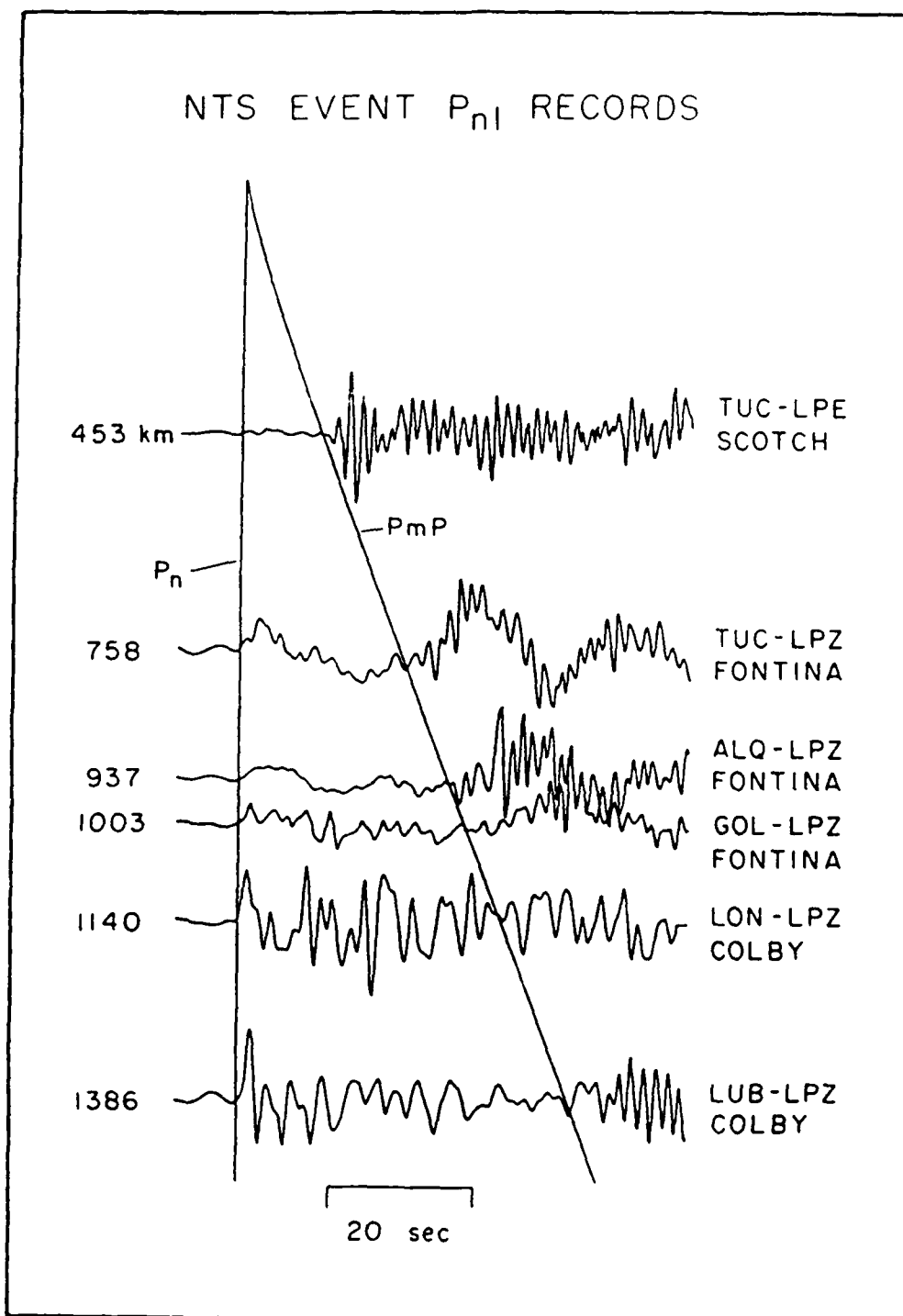
Figure 23. A long period seismic section of explosion records from the western U. S. The high frequency energy associated with the P_g phase is clear in both Figure 22 and 23 and commences with the PmP arrival.

usual, the long periods are fit extremely well, but so are many of the details at short periods. The signal appears deterministic down to periods perhaps as short as two seconds. We are not suggesting that this deterministic behavior holds up at high frequency, but we do suggest that Pnl type calculations might be used as a guide in identifying when information that is rich in discrimination potential is arriving in the record. We also conclude that our western U. S. studies of crustal resonance phases will be relevant to data from other tectonic environs.

Crustal Resonance Phases: It would be useful at this juncture to review some of the details associated with computation and analysis of crustal resonance phases. Just as in Pnl calculations, we assume a layer over a half space crustal model. A generalized ray representation of the response of the model is particularly well suited for determining exactly how arrivals such as crustal resonance phases are being excited. The Green's function can be built progressively by adding in more rays until the feature of interest emerges. Figure 26 shows the development of the Green's function for the Helmberger and Engen (1980) western U. S. crust model at a distance of 1000 km. It is being progressively constructed through sequential ray addition. Two of the four fundamental Green's functions are shown; vertical strike slip on the left and vertical dip slip on the right. These two fundamental Green's functions produce the most variable regional P waves because they have the strongest variation in vertical radiation pattern as shown at the top. The response to just the direct P and S waves is shown first. Then the effect of adding in those rays with just one reverberation in the crust along with their associated depth phases (PmP, pPmP, SmP, sSmP etc.)is shown. The third response is for two reverberations in the crust with depth phases, the fourth
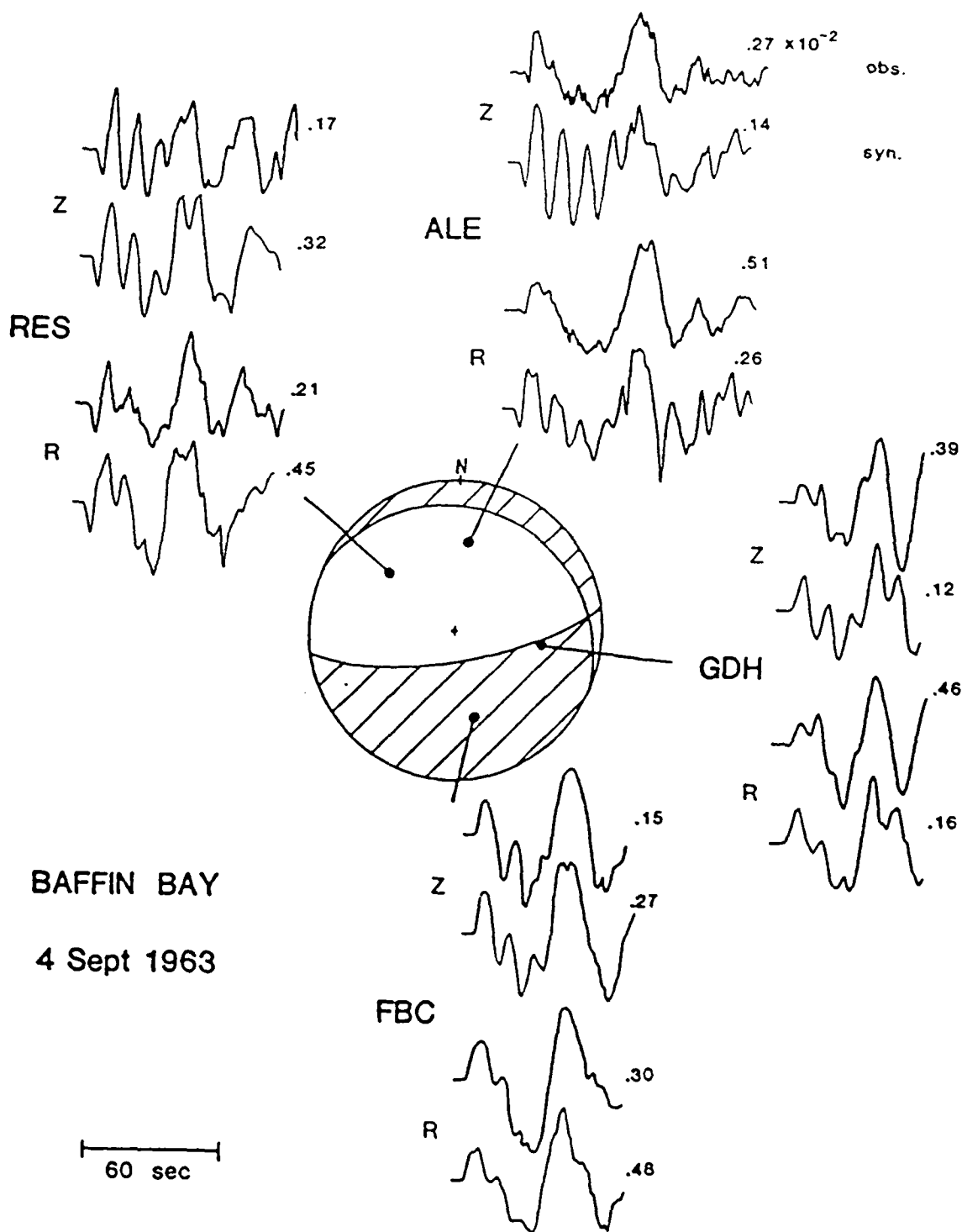
Figure 24. Observed and synthetic Pnl waveforms for the September 4, 1963 Baffin Bay earthquake. Peak to peak amplitudes in cm x 10^{-3} are shown.
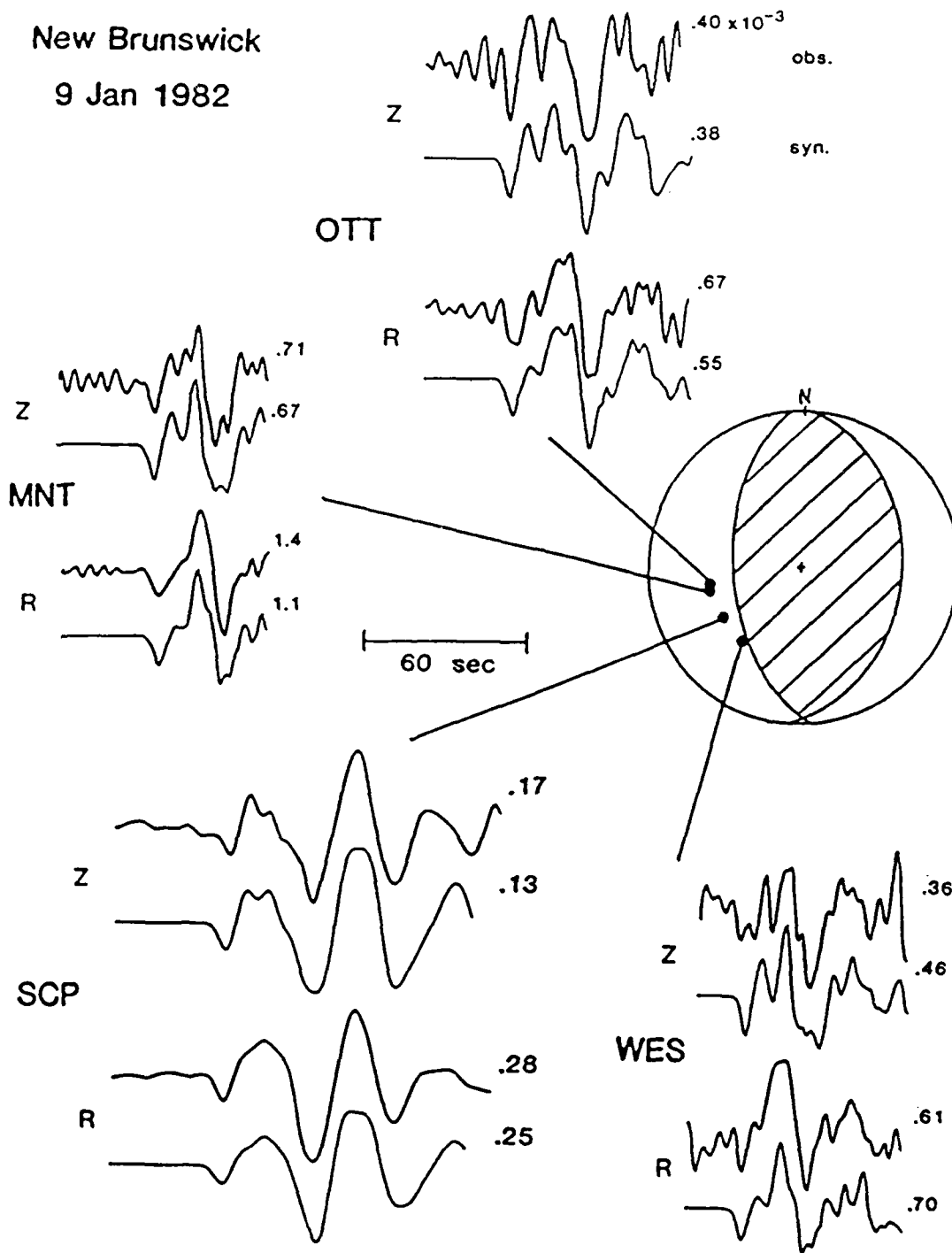
Figure 25. Observed and synthetic waveforms for the January 9, 1982 New Brunswick earthquake. Peak to peak amplitudes in cm x 10^{-3} are indicated.
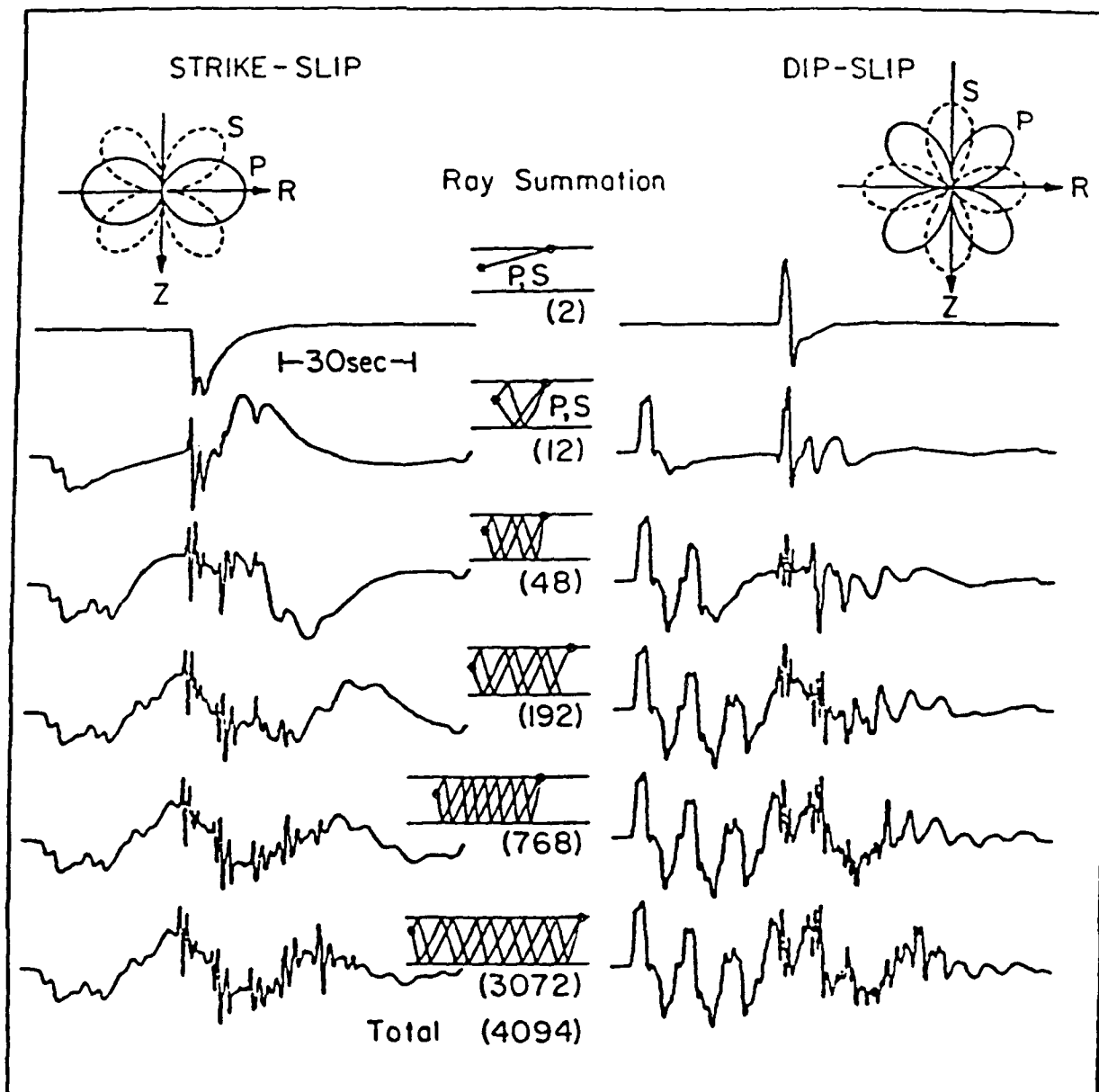
Figure 26. Green's functions for a layer over a half space computed using generalized rays. Successive rows are computed by adding in more crustal reverberations as indicated. The crustal resonance phases are high frequency arrivals commencing about half way through the trace.

for four and so on. The number of additional rays in each iteration is indicated. The number of rays grows so rapidly with each iteration that considering any more than 5 reverberations would be impractical. The crustal resonance phases are the periodic high frequency pulses commencing about half way through the trace. Successive resonance phases appear as successive reverberations of rays are added in. The long period oscillations that build up have classically been called PL.

Since it is clear that these reverberation phases exist, at least at moderate periods, it is natural to explore the possibility that they could be useful in discrimination. The use of ratios of phases for discrimination such as ratios of P_g to L_g, suggest a similar study of the ratio of the first to the second crustal resonance? In further work, we examined the composition of the first two resonance phases in terms of generalized rays in more detail. For an explosion the first resonance is almost completely made up of the three rays P, PmP and pPmP. Its high frequency is caused by the strong interference of PmP with the depth phase. The direct ray, P, contributes primarily long period energy. Interestingly, the second resonance phase is not dominated by rays with a complete extra reverberation in the crust, but by rays which have at least one converted leg. For an explosion, the rays are PmS, pSmS, PmPSmS, PmPSmP, and PmSPmP. Earthquakes would also contribute energy to the second resonance through SmS, sPmP and SmSPmP. However, it is important to bear in mind that this is high frequency regional data, and only stable properties of the data are important. As we will show in a later section, the first crustal resonance appears to be an efficient energy channel for P and the second

resonance for S. The best method for discriminating using P_g may be to look at the relative amount of scattered SV energy between the first and second resonance phases. There should be more scattered S in earthquakes.

The basic philosophy behind many discrimination studies has been to search for stronger S excitation than P for earthquakes in one pair of regional phases or another. The best known studies are probably those involving the ratio of P_g to Lg or P_n to S_n (Blandford, 1981; Dysart and Pulli, 1988). To those familiar with that work, it may seem strange to consider looking at the relative P and S excitation within just P_g. However, there are strong channels for energy that leaves the source as S into different crustal resonances and they differ from resonance to resonance. It is reasonable to expect a change in the amount of S energy between the first and second resonance and that the ratio of this energy will differ between explosions and earthquakes.

There is no doubt that crustal resonance phases exist in an idealized case. However, it remains to be established to what extent they exist and how coherent they are in a real crust at high frequency. To search for these phases, we used the same digital data base from ALQ and ANMO that we used in the P_n study discussed in the preceding, but concentrated on the P_g portion of the signal. Although there were some indications of a series of arrivals pumping energy into the P_g coda in some of the raw data, the effects of scattering and other variations between events seems to dominate. This has long been known to be the greatest difficulty in interpreting regional data. To suppress the scattering effects, we aligned the signals very carefully at

42

P_n time and summed. The Yucca and Pahute data were treated separately. This procedure neglects the difference in slowness between resonance phases and P_n, but our results indicate that this is a reasonable approach.

The results are shown in Figures 27 and 28 where we display progressive sums of records. Each subsequent line shows the effects of adding in an additional record. The final sums clearly indicate that there are coherent resonance phases at frequencies of several hz. There are 10 traces summed in the stack of Yucca events in Figure 27. The first two crustal resonance phases develop almost immediately indicating that they are very coherent. A third appears by the time 4 traces are added in and the sum has stabilized by the time 8 are added in. Actually, this is a relatively rapid rate of stabilization indicating that the resonance phases are very coherent for this path. In the Pahute record stack, the first and third resonance phases stabilize first, while the second does not really emerge clearly until 11 traces are added. At the bottom, we show a synthetic for a simple layer over a half space model just to show that the resonance phases have approximately the character we expect.

An important instrumentation change occurred at the ANMO station in about 1983. Two horizontal short period instruments were added which began to supply the necessary information for studying the relative polarization of crustal resonances. A limited number of explosions have been recorded so far. We have performed some preliminary analyses of this data. By simply inspecting the data, we have developed the impression that the first resonance is an efficient compressional energy channel and the second is much more favorable for shear. Figure 29 shows a good example of the effect we are

43

PROGRESSIVE SUM OF RECORDS
YUCCA TO ALQ OR ANMO

2 traces summed

4

6

10 sec

8 traces summed

Short Period Crustal
Resonance Phases

10
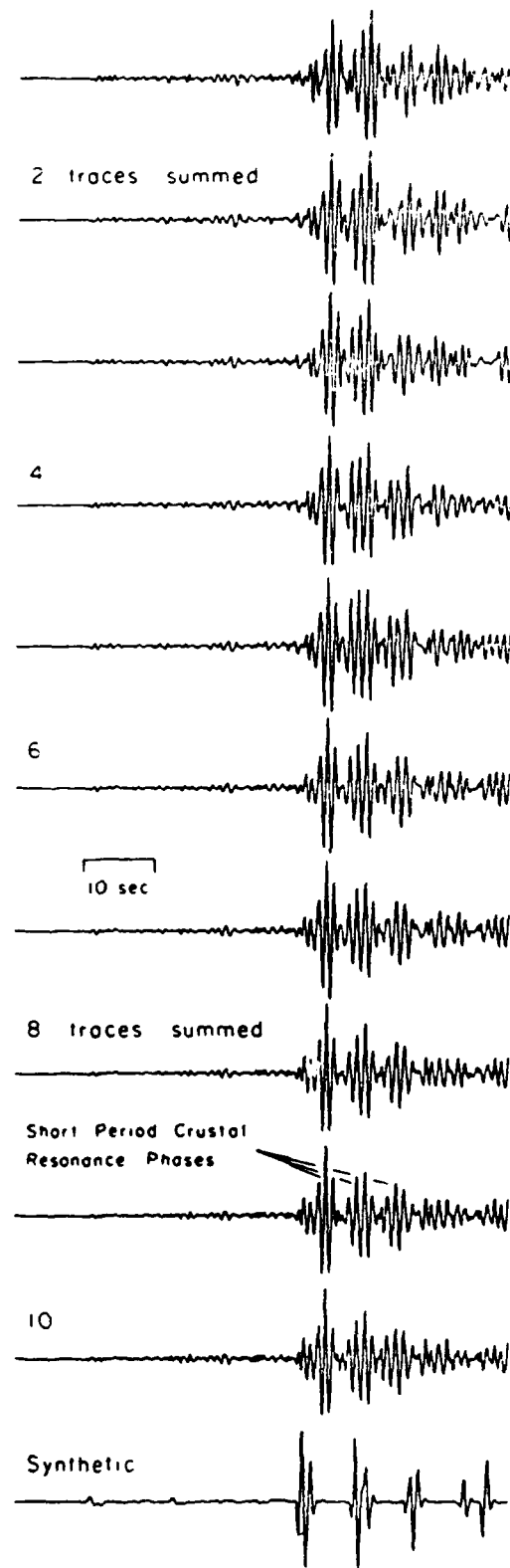
Synthetic

Figure 27. The crustal resonance phases for Yucca events are separated from the noise by stacking. The synthetic at the bottom merely indicates that the phases have approximately the right timing and amplitude.

PROGRESSIVE SUM OF RECORDS
PAHUTE TO ALO OR ANMO
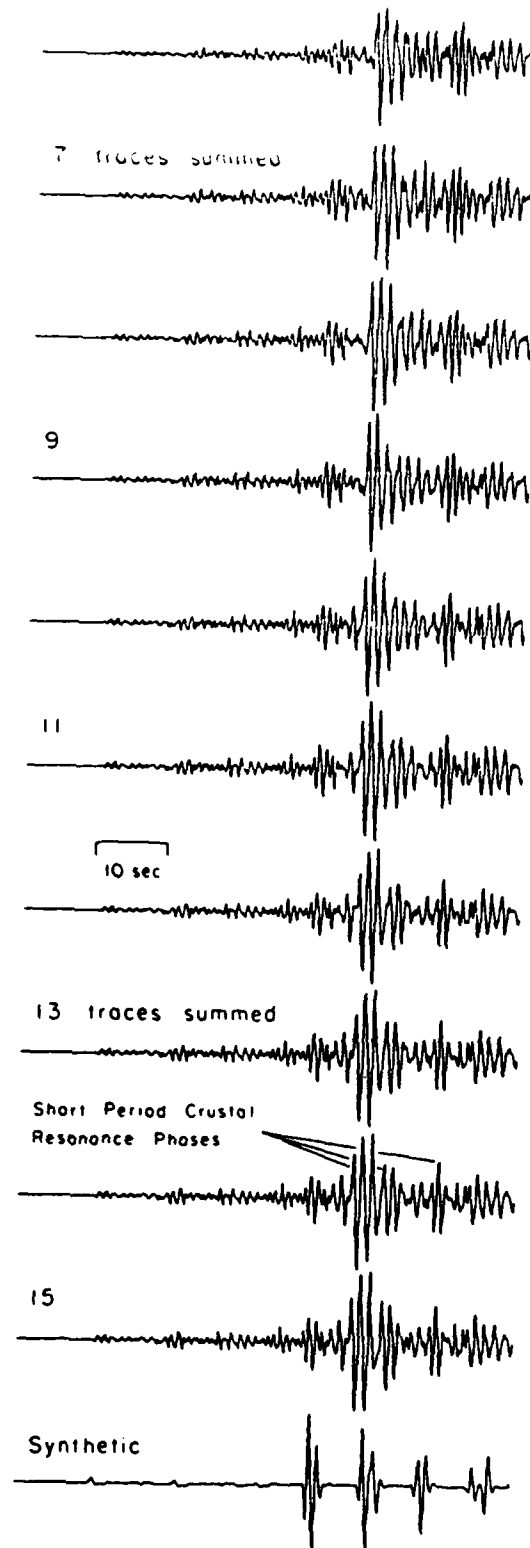
Figure 28. The crustal resonance phases for Pahute events are separated from the noise by stacking. The synthetic at the bottom merely indicates that the phases have approximately the right timing and amplitude.

45
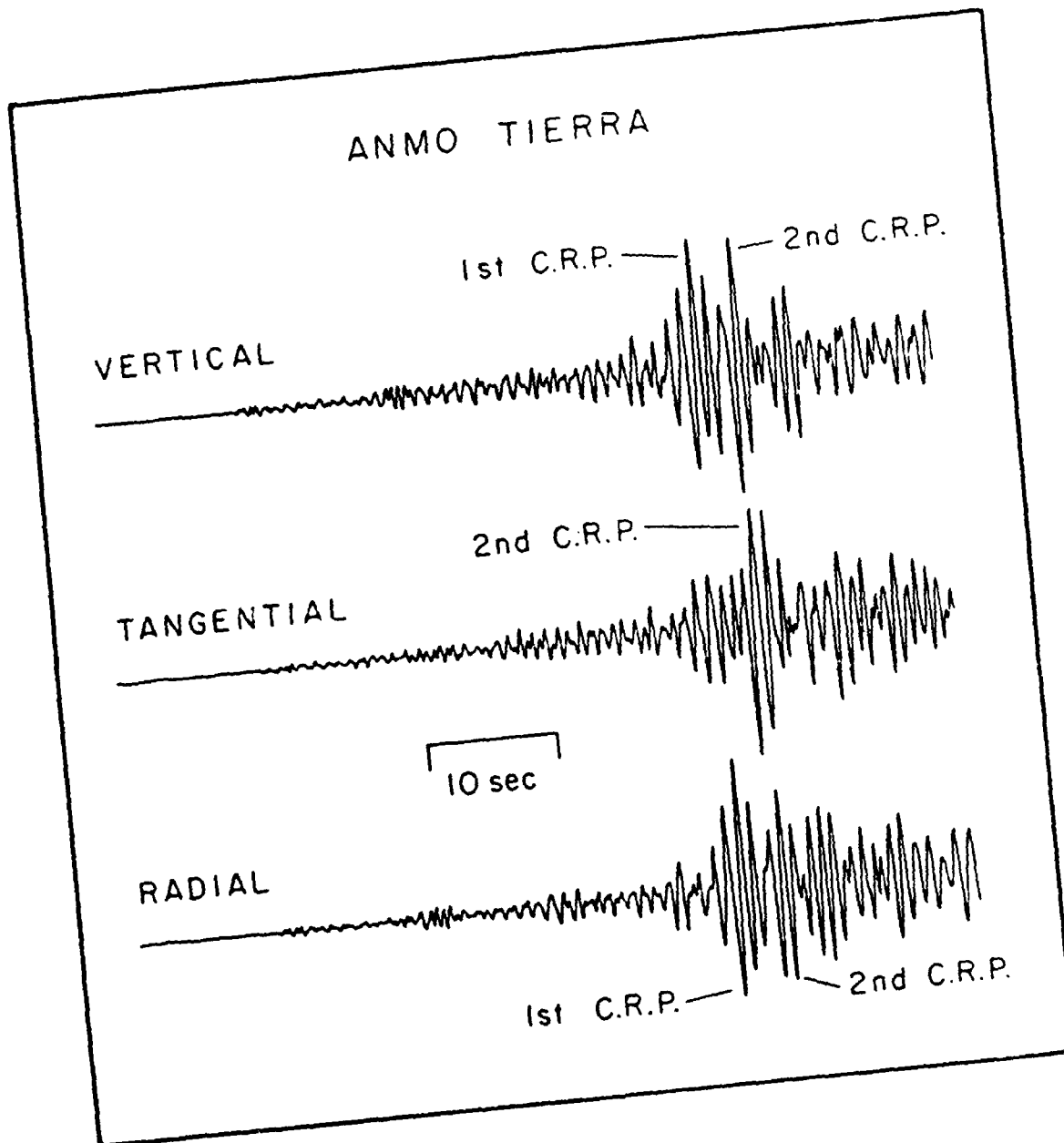
Figure 29. Three component observation at ANMO of a small Pahute event. Note the increase in the amount of S energy at the time of arrival of the second crustal resonance phase. This is presumed to be scattered SV.

seeing. In this particular instance, the crustal resonances are visible without stacking. They appear to be very similar on the radial and vertical. The second resonance is heavily favored on the tangential, however. This could not be true SH energy in the theoretical sense, but recalling that this is high frequency energy traveling in the real earth it could be interpreted as scattered S traveling in one or several of the favored shear modes.

The majority of the events for which we have data so far are from Pahute since those events are larger and trigger the instrument more consistently. We have rotated and stacked the traces of 10 events. The results are shown in Figure 30. On average, the second resonance is suppressed on the radial relative to either the vertical or tangential. The first is equally strong on all three. This is not inconsistent with the example shown in the previous figure. On average, there could be a component of off azimuth P on the tangential to account for the first arrival and then a consistent component of scattered S to account for the second. The suppression of the second resonance on the radial component is interesting because this is what is predicted by the synthetics shown on the bottom. The SV energy must approach the station at low apparent velocity and be concentrated on the vertical. The key point is that there is a clear evolution of particle motion between the first and second resonances. The questions ahead are can it be reliably measured for single events and can it be used to discriminate?

Another important type of information that can be resolved through the stacking procedure illustrated by Figure 27 regards the character of the signal generated noise in this type of data. The traces are all normalized to unit peak before stacking. The peak amplitudes of the sums after stacking are

47
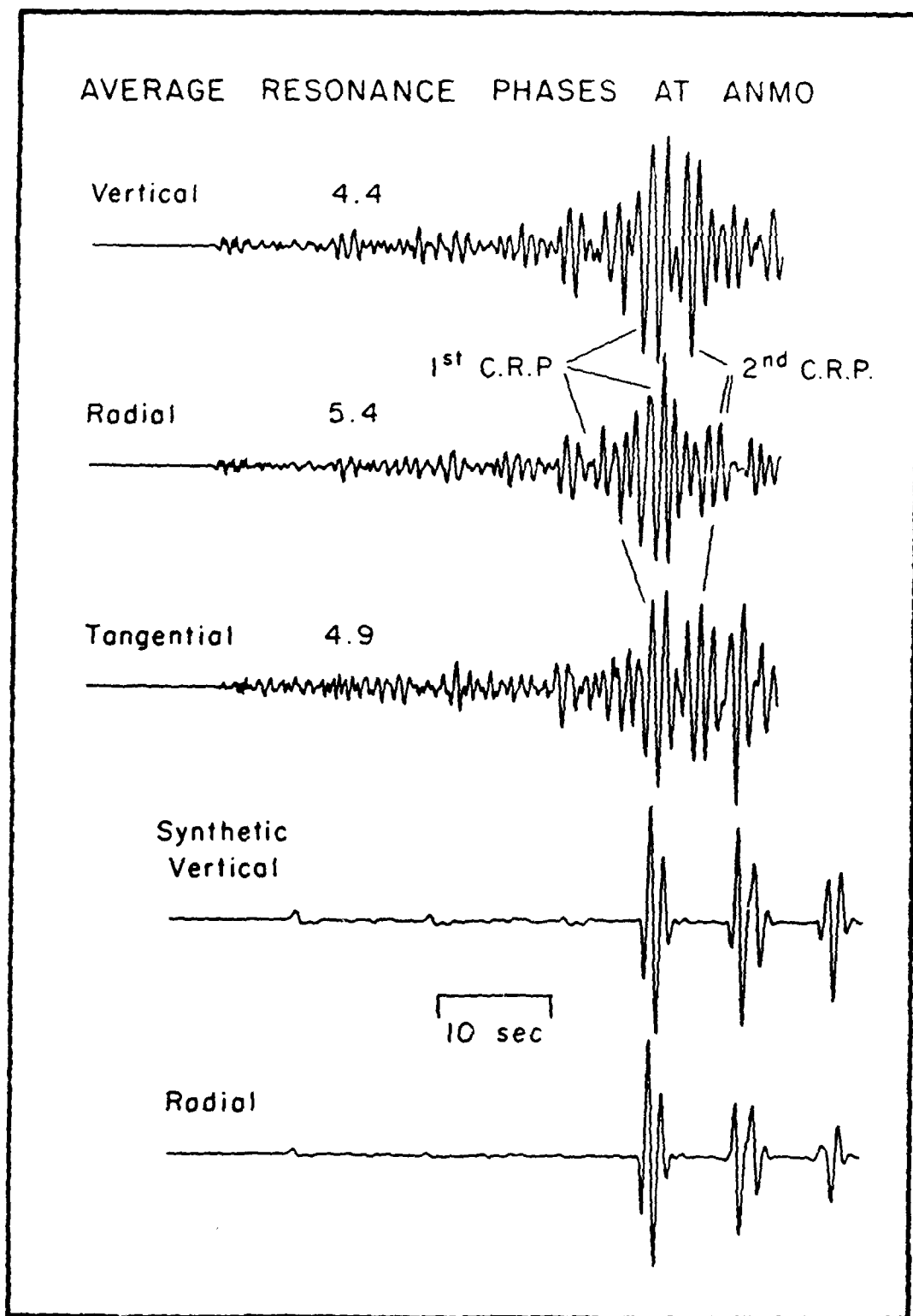
Figure 30. Average three component P_g waveforms for Pahute events at ANMO are determined by stacking. Note the evolution of particle motion between the first and second crustal resonance. A similar evolution is predicted in the synthetics.

indicated. The average peak Tangential/Radial prior to stacking was .515. After stacking it was only reduced to .351. There is a significant component of the energy in the P wave train that is both coherent and tangential. This type of noise data could be used in predicting the expected performance of discriminants that should work in theory.

DISCUSSION

There is little need to discuss the P_n discriminant further. It is simple in concept and design which makes the likelihood that it will work relatively high. The basic idea behind it is that at short times, before the depth phases from an earthquake could possibly arrive, the explosion waveform differs systematically from the earthquake because its depth phases have arrived.

The P_g discriminant is in a much earlier phase of development than the P_n, but the stacking experiments show that there is a strong basis for further work. Deterministic calculations in highly idealized crust models have played an important role in the analysis of the discriminant presented here. It is important to note that it is not intended that such calculations will play a direct role in the actual application of the discriminant. They are now only being used as a tool for interpretation of the stacked data to help guide in choosing which features of regional arrivals are most likely to differ between earthquakes and explosions.

It would seem that most researchers who have dealt with high frequency regional data have rapidly abandoned a forward modeling approach to data interpretation and taken a purely empirical approach. There are many good reasons for this. The basic principles which apply at periods longer than a second clearly break down in a severe way at higher frequency. The duration of regional phases is much longer than the possible duration of the source, and coupling between the radial and tangential components is very strong. In this work, we have shown through stacking of the P_g complex that on average it is made up of a series of coherent subpulses which individually do have

reasonable durations. The synthetic seismogram modeling allows interpretation of the pulses as crustal resonance phases. The continuing arrival of these pulses along with a reasonable amount of coda account for the overall duration of the P_g complex. Thus, though the calculations are highly idealized, they have provided an important guide to interpretation. The calculations also indicate that there are strong channels for S into the P_g phase and for P into the S_g - Lg complex. These channels may account for why the P_g to Lg discriminant performs poorly. However, it would also appear that the ratios of the first to second resonance phase may constitute the basis for a discriminant. No forward synthetics would be involved in the actual implementation of the discriminant. This would require sophisticated phase detectors and particle motion filters which would measure average properties of P_g with time.

CONCLUSIONS

The overall purpose of this work is to develop and test regional discriminants in the western U. S. and then to investigate how reliably they can be transported to other areas where earth structure and tectonic conditions might be much different. The P_n waveform discriminant has been developed in principle. Future efforts need to be directed towards measuring additional average P_n waveforms at digital stations in the western U. S. The P_g discriminant is in a much more primitive state. Additional studies are needed to fully characterize crustal resonance phases with particular attention being paid to relative particle motion. The studies of Pnl in the eastern U. S. and Canadian shield indicate that these resonances are pervasive phenomena, and if a discriminant can be developed, it should be highly transportable. We note, in this regard, that Vogfjord and Langston (1988) have already reported the detection of what are probably resonance phases at NORESS. They called them P_{g1} and P_{g2} however.

REFERENCES

Blandford, R. R., "Seismic discrimination problems at regional distances", in Identification of Seismic Sources, E. S. Husebye and S. Mykkelveit eds., D. Reidel Publishing Co., Dordrecht, The Netherlands, 695-740, 1981.

Burdick, L. J., "Estimation of the frequency dependence of Q from ScP and ScS phases", Geophys. J. R. A. S., 80, 35-55, 1985.

Burdick, L. J., and G. R. Mellman, "Inversion of the body waves of the Borrego Mountain Earthquake to the source mechanism", Bull. Seism. Soc. Am., 66, 1485-1499, 1976.

Burdick, L. J. and D. V. Helmberger, "The discrimination potential of crustal resonance phases", AFGL-TR-88-0054, ADA196096, 1988.

Burdick, L. J., T. C. Wallace and T. Lay, "Modeling the near field and teleseismic observations from the Amchitka test site", J. Geophys. Res., 89, 4373-4388, 1984a.

Burdick, L. J., T. Lay, D. V. Helmberger and D. G. Harkrider, "Implications of records from the spall zone of the Amchitka tests to nonlinear losses in the source region and to elastic radiation from spall", Woodward Clyde Consultants Report, WCCP-R-84-03, Woodward Clyde Consultants, Pasadena, CA., 1984b.

Dysart, P. and J. Pulli, "Waveform and spectral characteristics of regional earthquakes and chemical explosions recorded at the NORESS array, in R&D Support for the Center for Seismic Studies: Final Report Technical report C88-01, January 1988, Center for Seismic Studies, Arlington Virginia, 1988.

Hartzell, S. H., L. J. Burdick and T. Lay, "Effective source functions for Pahute Mesa nuclear tests", Woodward Clyde Consultants Report, WCCP-83-03, Woodward Clyde Consultants, Pasadena, CA, 1983.

Helmberger, D. V. and G. R. Engen, "Modeling the long period body waves from shallow earthquakes at regional ranges", Bull. Seism. Soc. Am., 70, 1699-1714, 1980.

Murphy, J. R. and T. J. Bennett, "A discrimination analysis of short period regional seismic data recorded at Tonto Forest Observatory", Bull. Seism. Soc. Am., 72, 1351-1366, 1982.

Vogfjord, K. S. and C. A. Langston, "Short period regional phases recorded at NORESS", EOS. Trans. Am. Geophys. Un., 69, 408, 1988.

Wallace, T. C., D. V. Helmberger and G. R. Engen, "Evidence of tectonic release from underground nuclear explosions in long period P waves", Bull. Seism. Soc. Am., 73, 593-613, 1983.

CONTRACTORS (United States)

Professor Keiiti Aki
Center for Earth Sciences
University of Southern California
University Park
Los Angeles, CA 90089-0741

Professor Charles B. Archambeau
Cooperative Institute for Resch
   in Environmental Sciences
University of Colorado
Boulder, CO 80309

Dr. Thomas C. Bache Jr.
Science Applications Int'l Corp.
10210 Campus Point Drive
San Diego, CA 92121   (2 copies)

Dr. Douglas R. Baumgardt
Signal Analysis & Systems Div.
ENSCO, Inc.
5400 Port Royal Road
Springfield, VA 22151-2388

Dr. S. Bratt
Science Applications Int'l Corp.
10210 Campus Point Drive
San Diego, CA 92121

Dr. Lawrence J. Burdick
Woodward-Clyde Consultants
P.O. Box 93245
Pasadena, CA 91109-3245 (2 copies)

Professor Robert W. Clayton
Seismological Laboratory/Div. of
   Geological & Planetary Sciences
California Institute of Technology
Pasadena, CA 91125

Dr Karl Cogan
N. E. Research
P.O. Box 857
Norwich, VT 05055

Dr. Vernon F. Cormier
Department of Geology & Geophysics
U-45, Roon 207
The University of Conneticut
Storrs, Connecticut 06268

Dr. Zoltan A. Der
ENSCO, Inc.
5400 Port Royal Road
Springfield, VA 22151-2388

Professor John Ferguson
Center for Lithospheric Studies
The University of Texas at Dallas
P.O. Box 830688
Richardson, TX 75083-0688

Professor Stanley Flatte'
Applied Sciences Building
University of California, Santa Cruz
Santa Cruz, CA 95064

Professor Steven Grand
Department of Geology
245 Natural History Building
1301 West Green Street
Urbana, IL 61801

Professor Roy Greenfield
Geosciences Department
403 Deike Building
The Pennsylvania State University
University Park, PA 16802

Professor David G. Harkrider
Seismological Laboratory
Div of Geological & Planetary Sciences
California Institute of Technology
Pasadena, CA 91125

Professor Donald V. Helmberger
Seismological Laboratory
Div of Geological & Planetary Sciences
California Institute of Technology
Pasadena, CA 91125

Professor Eugene Herrin
Institute for the Study of Earth
 & Man/Geophysical Laboratory
Southern Methodist University
Dallas, TX 75275

Professor Robert B. Herrmann
Department of Earth & Atmospheric
       Sciences
Saint Louis University
Saint Louis, MO 63156

Professor Lane R. Johnson
Seismographic Station
University of California
Berkeley, CA 94720

Professor Thomas H. Jordan
Department of Earth, Atmospheric
 and Planetary Sciences
Mass Institute of Technology
Cambridge, MA 02139

Dr Alan Kafka
Department of Geology &
  Geophysics
Boston College
Chestnut Hill, MA 02167

Professor Leon Knopoff
University of California
Institute of Geophysics
  & Planetary Physics
Los Angeles, CA 90024

Professor Charles A. Langston
Geosciences Department
403 Deike Building
The Pennsylvania State University
University Park, PA 16802

Professor Thorne Lay
Department of Geological Sciences
1006 C.C. Little Building
University of Michigan
Ann Harbor, MI 48109-1063

Dr. Randolph Martin III
New England Research, Inc.
P.O. Box 857
Norwich, VT 05055

Dr. Gary McCartor
Mission Research Corp.
735 State Street
P.O. Drawer 719
Santa Barbara, CA 93102   (2 copies)

Professor Thomas V. McEvilly
Seismographic Station
University of California
Berkeley, CA 94720

Dr. Keith L. McLaughlin
S-CUBED,
A Division of Maxwell Laboratory
P.O. Box 1620
La Jolla, CA 92038-1620

Professor William Menke
Lamont-Doherty Geological Observatory
  of Columbia University
Palisades, NY 10964

Professor Brian J. Mitchell
Department of Earth & Atmospheric
     Sciences
Saint Louis University
Saint Louis, MO 63156

Mr. Jack Murphy
S-CUBED
A Division of Maxwell Laboratory
11800 Sunrise Valley Drive
Suite 1212
Reston, VA 22091 (2 copies)

Professor J. A. Orcutt
Institute of Geophysics and Planetary
  Physics, A-205
Scripps Institute of Oceanography
Univ. of California, San Diego
La Jolla, CA 92093

Professor Keith Priestley
University of Nevada
Mackay School of Mines
Reno, NV 89557

Wilmer Rivers
Teledyne Geotech
314 Montgomery Street
Alexandria, VA 22314

Professor Charles G. Sammis
Center for Earth Sciences
University of Southern California
University Park
Los Angeles, CA 90089-0741

Dr. Jeffrey L. Stevens
S-CUBED,
A Division of Maxwell Laboratory
P.O. Box 1620
La Jolla, CA 92038-1620

Professor Brian Stump
Institute for the Study of Earth & Man
Geophysical Laboratory
Southern Methodist University
Dallas, TX 75275

Professor Ta-liang Teng
Center for Earth Sciences
University of Southern California
University Park
Los Angeles, CA 90089-0741

Professor M. Nafi Toksoz
Earth Resources Lab
Dept of Earth, Atmospheric and
     Planetary Sciences
Massachusetts Institute of Technology
42 Carleton Street
Cambridge, MA 02142

Professor Terry C. Wallace
Department of Geosciences
Building #11
University of Arizona
Tucson, AZ 85721

Weidlinger Associates
ATTN: Dr. Gregory Wojcik
620 Hansen Way, Suite 100
Palo Alto, CA 94304
Professor Francis T. Wu
Department of Geological Sciences
State University of new York
 At Binghamton
Vestal, NY 13901

Dr. Monem Abdel-Gawad
Rockwell Internat'l Science Center
1049 Camino Dos Rios
Thousand Oaks, CA 91360

Professor Shelton S. Alexander
Geosciences Department
403 Deike Building
The Pennsylvania State University
University Park, PA 16802

Dr. Ralph Archuleta
Department of Geological
  Sciences
Univ. of California at
  Santa Barbara
Santa Barbara, CA

Dr. Muawia Barazangi
Geological Sciences
Cornell University
Ithaca, NY 14853

J. Barker
Department of Geological Sciences
State University of New York
 at Binghamton
Vestal, NY 13901

Mr. William J. Best
907 Westwood Drive
Vienna, VA 22180

Dr. N. Biswas
Geophysical Institute
University of Alaska
Fairbanks, AK 99701

Dr. G. A. Bollinger
Department of Geological Sciences
Virginia Polytechnical Institute
21044 Derring Hall
Blacksburg, VA 24061

Dr. James Bulau
Rockwell Int'l Science Center
1049 Camino Dos Rios
P.O. Box 1085
Thousand Oaks, CA 91360

Mr. Roy Burger
1221 Serry Rd.
Schenectady, NY 12309

Dr. Robert Burridge
Schlumberger-Doll Resch Ctr.
Old Quarry Road
Ridgefield, CT 06877

Science Horizons, Inc.
ATTN: Dr. Theodore Cherry
710 Encinitas Blvd., Suite 101
Encinitas, CA 92024 (2 copies)

Professor Jon F. Claerbout
Professor Amos Nur
Dept. of Geophysics
Stanford University
Stanford, CA 94305 (2 copies)

Dr. Anton W. Dainty
AFGL/LWH
Hanscom AFB, MA 01731

Dr. Steven Day
Dept. of Geological Sciences
San Diego State U.
San Diego, CA 92182

Professor Adam Dziewonski
Hoffman Laboratory
Harvard University
20 Oxford St.
Cambridge, MA 02138

Professor John Ebel
Dept of Geology & Geophysics
Boston College
Chestnut Hill, MA 02167

Dr. Alexander Florence
SRI International
333 Ravenswood Avenue
Menlo Park, CA 94025-3493

Dr. Donald Forsyth
Dept. of Geological Sciences
Brown University
Providence, RI 02912

Dr. Anthony Gangi
Texas A&M University
Department of Geophysics
College Station, TX 77843

Dr. Freeman Gilbert
Institute of Geophysics &
  Planetary Physics
Univ. of California, San Diego
P.O. Box 109
La Jolla, CA 92037

Mr. Edward Giller
Pacific Seirra Research Corp.
1401 Wilson Boulevard
Arlington, VA 22209

Dr. Jeffrey W. Given
Sierra Geophysics
11255 Kirkland Way
Kirkland, WA 98033

Dr. Henry L. Gray
Associate Dean of Dedman College
Department of Statistical Sciences
Southern Methodist University
Dallas, TX 75275

Rong Song Jih
Teledyne Geotech
314 Montgomery Street
Alexandria, Virginia 22314

Professor F.K. Lamb
University of Illinois at
  Urbana-Champaign
Department of Physics
1110 West Green Street
Urbana, IL 61801

Dr. Arthur Lerner-Lam
Lamont-Doherty Geological Observatory
 of Columbia University
Palisades, NY 10964

Dr. L. Timothy Long
School of Geophysical Sciences
Georgia Institute of Technology
Atlanta, GA 30332

Dr. Peter Malin
University of California at Santa Barbara
Institute for Central Studies
Santa Barbara, CA 93106

Dr. George R. Mellman
Sierra Geophysics
11255 Kirkland Way
Kirkland, WA 98033

Dr. Bernard Minster
 Institute of Geophysics and Planetary
  Physics, A-205
Scripps Institute of Oceanography
Univ. of California, San Diego
La Jolla, CA 92093

Professor John Nabelek
College of Oceanography
Oregon State University
Corvallis, OR 97331

Dr. Geza Nagy
U. California, San Diego
Dept of Ames, M.S. B-010
La Jolla, CA 92093

Dr. Jack Oliver
Department of Geology
Cornell University
Ithaca, NY 14850

Dr. Robert Phinney/Dr. F.A. Dahlen
Dept of Geological
 Geophysical Sci. University
Princeton University
Princeton, NJ 08540 (2 copies)

RADIX Systems, Inc.
Attn: Dr. Jay Pulli
2 Taft Court, Suite 203
Rockville, Maryland 20850

Professor Paul G. Richards
Lamont-Doherty Geological
 Observatory of Columbia Univ.
Palisades, NY 10964

Dr. Norton Rimer
S-CUBED
A Division of Maxwell Laboratory
P.O. 1620
La Jolla, CA 92038-1620

Professor Larry J. Ruff
Department of Geological Sciences
1006 C.C. Little Building
University of Michigan
Ann Arbor, MI 48109-1063

Dr. Alan S. Ryall, Jr.
Center of Seismic Studies
1300 North 17th Street
Suite 1450
Arlington, VA 22209-2308   (4 copies)

Dr. Richard Sailor
TASC Inc.
55 Walkers Brook Drive
Reading, MA 01867

Thomas J. Sereno, Jr.
Service Application Int'l Corp.
10210 Campus Point Drive
San Diego, CA 92121

Dr. David G. Simpson
Lamont-Doherty Geological Observ.
 of Columbia University
Palisades, NY 10964

Dr. Bob Smith
Department of Geophysics
University of Utah
1400 East 2nd South
Salt Lake City, UT 84112

Dr. S. W. Smith
Geophysics Program
University of Washington
Seattle, WA 98195

Dr. Stewart Smith
IRIS Inc.
1616 N. Fort Myer Drive
Suite 1440
Arlington, VA 22209

Rondout Associates
ATTN: Dr. George Sutton,
Dr. Jerry Carter, Dr. Paul Pomeroy
P.O. Box 224
Stone Ridge, NY 12484 (4 copies)

Dr. L. Sykes
Lamont Doherty Geological Observ.
Columbia University
Palisades, NY 10964

Dr. Pradeep Talwani
Department of Geological Sciences
University of South Carolina
Columbia, SC 29208

Dr. R. B. Tittmann
Rockwell International Science Center
1049 Camino Dos Rios
P.O. Box 1085
Thousand Oaks, CA 91360

Professor John H. Woodhouse
Hoffman Laboratory
Harvard University
20 Oxford St.
Cambridge, MA 02138

Dr. Gregory B. Young
ENSCO, Inc.
5400 Port Royal Road
Springfield, VA 22151-2388

Dr. Peter Basham
Earth Physics Branch
Geological Survey of Canada
1 Observatory Crescent
Ottawa, Ontario
CANADA K1A OY3

Dr. Eduard Berg
Institute of Geophysics
University of Hawaii
Honolulu, HI 96822

Dr. Michel Bouchon - Universite
  Scientifique et Medicale de Grenob
Lab de Geophysique - Interne et
  Tectonophysique - I.R.I.G.M-B.P.
38402 St. Martin D'Heres
Cedex FRANCE

Dr. Hilmar Bungum/NTNF/NORSAR
P.O. Box 51
Norwegian Council of Science,
Industry and Research, NORSAR
N-2007 Kjeller, NORWAY

Dr. Michel Campillo
I.R.I.G.M.-B.P. 68
38402 St. Martin D'Heres
Cedex, FRANCE

Dr. Kin-Yip Chun
Geophysics Division
Physics Department
University of Toronto
Ontario, CANADA M5S 1A7

Dr. Alan Douglas
Ministry of Defense
Blacknest, Brimpton,
  Reading RG7-4RS
UNITED KINGDOM

Dr. Manfred Henger
Fed. Inst. For Geosciences & Nat'l Res.
Postfach 510153
D-3000 Hannover 51
FEDERAL REPUBLIC OF GERMANY

Dr. E. Husebye
NTNF/NORSAR
P.O. Box 51
N-2007 Kjeller, NORWAY

Ms. Eva Johannisson
Senior Research Officer
National Defense Research Inst.
P.O. Box 27322
S-102 54 Stockholm
SWEDEN

Tormod Kvaerna
NTNF/NORSAR
P.O. Box 51
N-2007 Kjeller, NORWAY

Mr. Peter Marshall, Procurement
  Executive, Ministry of Defense
Blacknest, Brimpton,
  Reading FG7-4RS
UNITED KINGDOM (3 copies)

Dr. Ben Menaheim
Weizman Institute of Science
Rehovot, ISRAEL 951729

Dr. Svein Mykkeltveit
NTNF/NORSAR
P.O. Box 51
N-2007 Kjeller, NORWAY (3 copies)

Dr. Robert North
Geophysics Division
Geological Survey of Canada
1 Observatory crescent
Ottawa, Ontario
CANADA, K1A OY3

Dr. Frode Ringdal
NTNF/NORSAR
P.O. Box 51
N-2007 Kjeller, NORWAY

Dr. Jorg Schlittenhardt
Federal Inst. for Geosciences & Nat'l Res.
Postfach 510153
D-3000 Hannover 51
FEDERAL REPUBLIC OF GERMANY

University of Hawaii
Institute of Geophysics
ATTN: Dr. Daniel Walker
Honolulu, HI 96822

Dr. Ramon Cabre, S.J.
c/o Mr. Ralph Buck
Economic Consular
American Embassy
APO Miami, Florida 34032

Professor Peter Harjes
Institute for Geophysik
Rhur University/Bochum
P.O. Box 102148, 4630 Bochum 1
FEDERAL REPUBLIC OF GERMANY

Professor Brian L.N. Kennett
Research School of Earth Sciences
Institute of Advanced Studies
G.P.O. Box 4
Canberra 2601
AUSTRALIA

Dr. B. Massinon
Societe Radiomana
27, Rue Claude Bernard
7,005, Paris, FRANCE (2 copies)

Dr. Pierre Mechler
Societe Radiomana
27, Rue Claude Bernard
75005, Paris, FRANCE

GOVERNMENT

Dr. Ralph Alewine III
DARPA/NMRO
1400 Wilson Boulevard
Arlington, VA 22209-2308

Dr. Robert Blandford
DARPA/NMRO
1400 Wilson Boulevard
Arlington, VA 22209-2308

Sandia National Laboratory
ATTN: Dr. H. B. Durham
Albuquerque, NM 87185

Dr. Jack Evernden
USGS-Earthquake Studies
345 Middlefield Road
Menlo Park, CA 94025

U.S. Geological Survey
ATTN: Dr. T. Hanks
Nat'l Earthquake Resch Center
345 Middlefield Road
Menlo Park, CA 94025

Dr. James Hannon
Lawrence Livermore Nat'l Lab.
P.O. Box 808
Livermore, CA 94550

U.S. Arms Control & Disarm. Agency
ATTN: Dick Morrow
Washington, D.C. 20451

Paul Johnson
ESS-4, Mail Stop J979
Los Alamos National Laboratory
Los Alamos, NM 87545

Ms. Ann Kerr
DARPA/NMRO
1400 Wilson Boulevard
Arlington, VA 22209-2308

Dr. Max Koontz
US Dept of Energy/DP 331
Forrestal Building
1000 Independence Ave.
Washington, D.C. 20585

AFOSR/NP
ATTN: Colonel Jerry J. Perrizo
Bldg 410
Bolling AFB, Wash D.C. 20332-6448

HQ AFTAC/TT
Attn: Dr. Frank F. Pilotte
Patrick AFB, Florida 32925-6001

Mr. Jack Rachlin
USGS - Geology, Rm 3 C136
Mail Stop 928 National Center
Reston, VA 22092

Robert Reinke
AFWL/NTESG
Kirtland AFB, NM 87117-6008

HQ AFTAC/TGR
Attn: Dr. George H. Rothe
Patrick AFB, Florida 32925-6001

Donald L. Springer
Lawrence Livermore National Laboratory
P.O. Box 808, L-205
Livermore, CA 94550

Dr. Lawrence Turnbull
OSWR/NED
Central Intelligence Agency
CIA, Room 5G48
Washington, D.C. 20505

Dr. Thomas Weaver
Los Alamos Scientific Laboratory
Los Almos, NM 97544

AFGL/SULL
Research Library
Hanscom AFB, MA 01731-5000 (2 copies)

Secretary of the Air Force (SAFRD)
Washington, DC 20330
Office of the Secretary Defense
DDR & E
Washington, DC 20330

HQ DNA
ATTN: Technical Library
Washington, DC 20305

Director, Technical Information
DARPA
1400 Wilson Blvd.
Arlington, VA 22209

AFGL/XO
Hanscom AFB, MA 01731-5000

Dr. W. H. K. Lee
USGS
Office of Earthquakes, Volcanoes,
  & Engineering
Branch of Seismology
345 Middlefield Rd
Menlo Park, CA 94025

Dr. William Leith
USGS
Mail Stop 928
Reston, VA 22092

Dr. Richard Lewis
Dir. Earthquake Engineering and
  Geophysics
U.S. Army Corps of Engineers
Box 631
Vicksburg, MS 39180

Dr. Robert Masse'
Box 25046, Mail Stop 967
Denver Federal Center
Denver, Colorado 80225

R. Morrow
ACDA/VI
Room 5741
320 21st Street N.W.
Washington, D.C. 20451

Dr. Keith K. Nakanishi
Lawrence Livermore National Laboratory
P.O. Box 808, L-205
Livermore, CA 94550 (2 copies)

Dr. Carl Newton
Los Alamos National Lab.
P.O. Box 1663
Mail Stop C335, Group E553
Los Alamos, NM 87545

Dr. Kenneth H. Olsen
Los Alamos Scientific Lab.
Post Office Box 1663
Los Alamos, NM 87545

Howard J. Patton
Lawrence Livermore National Laboratory
P.O. Box 808, L-205
Livermore, CA 94550

Mr. Chris Paine
Office of Senator Kennedy
SR 315
United States Senate
Washington, D.C. 20510

AFGL/LW
Hanscom AFB, MA 01731-5000

DARPA/PM
1400 Wilson Boulevard
Arlington, VA 22209

Defense Technical
  Information Center
Cameron Station
Alexandria, VA 22314
(5 copies)

Defense Intelligence Agency
Directorate for Scientific &
  Technical Intelligence
Washington, D.C. 20301

Defense Nuclear Agency/SPSS
ATTN: Dr. Michael Shore
6801 Telegraph Road
Alexandria, VA 22310

AFTAC/CA (STINFO)
Patrick AFB, FL 32925-6001

Dr. Gregory van der Vink
Congress of the United States
Office of Technology Assessment
Washington, D.C. 20510

Mr. Alfred Lieberman
ACDA/VI-OA'State Department Building
Room 5726
320 - 21St Street, NW
Washington, D.C. 20451